HIGH THROUGHAPUT METHOD FOR HYDROGEN PERMEABILITY MEASUREMENT OF PD ALLOY MEMBRANES

A Thesis

Presented to the Faculty of the Graduate School

of Cornell University

In Partial Fulfillment of the Requirements for the Degree of

Master of Science

by

Boyu Guo

August 2017

ABSTRACT

Hydrogen is a promising source for future energy because of its energy density, low emission, and the ability to be obtained from various sources. The development of a Pd alloy that has high H_2 permeability and low cost is desired as people are looking for cost-effective method for H_2 separation. We present a method that utilizes hydrogenography and yttrium indicator to perform simultaneous analysis of H_2 permeability of 89 different compositions of Pd alloy. Sputtering deposition and photolithography processing are used to prepare the samples, while Hough transformation is used to analyze the expansion of color changed area on the indicator and calculate the hydrogen permeability of the test material. The validity of our method is checked using pure Pd, and the results of PdCu alloy, PdRu alloy, PdMo alloy, and PdAgAu alloy are presented. It is observed that in PdRu alloy that a high Pd concentration leads to high hydrogen permeability. The same behavior was observed in PdCu alloy, but the hydrogen dissociation reaction is turned off when Cu concentration is higher than 20at.%. The addition of Mo to Pd shuts down the diffusion of hydrogen atoms inside the test material. In PdAgAu alloy high Pd concentration shows high hydrogen permeability, but the permeability drops quickly with the decrease in Pd concentration, and the hydrogen dissociation reaction shuts down when the Pd concentration drops below 35at.%.

BIOGRAPHICAL SKETCH

Boyu was interested in science from his childhood, when he wanted to become an astronaut or an astronomer. His interests shifted to materials science during high school when he decided he wants to develop something new but related to peoples' daily lives. He began his undergraduate studies in Materials Science and Engineering at Purdue University in August 2011. MSE at Purdue University focuses on metal and ceramic processing, and Boyu's research experience there is mostly related to metals. He got his bachelor's degree in May 2015.

Boyu's undergraduate studies granted him a strong basis in materials science. Although his study experience concentrates on metals, he was eager to learn new things and gain more experience on research. He joined Prof. van Dover's group at Cornell University to pursue his interests in renewable energy and new materials. Two years of research and study equipped him with knowledge and skills in thin film processing as well as data analysis. Pressing the research forward granted him lab experiences, problem solving experiences, inspired him to do more research, prepared him well for the future study and work.

After graduation, Boyu will start his Ph.D. studies in Materials Science at North Carolina State University.

ACKNOWLEDGEMENTS

I need to thank my graduate committee: Prof. Bruce van Dover and Prof. Jin Suntivich for their guidance through the duration of this project. Prof. van Dover was always available to help me solve problems with the development of experiment procedure, interpret unusual observations, and provide insight in data analysis. Prof. Suntivich was always happy to sit down with me and discuss the problem I was having in my project.

I also need to express my gratitude to members of van Dover research group for their help through this project. I would like to thank the PhD students, Abbigail van Wassen and Marc Murphy, who helped me to get started on vacuum technology and sputtering system as well as the trouble shooting when the systems were down. I would also like to thank Lewis Harbor, an undergraduate student for his help in the data analysis part of the project and Christopher Mizzi for setting up the theoretic basis for this project. The work in this project is partially performed in Cornell Nanoscale Facility (CNF).

Last and the most foremost, my parents and the rest of my family for their support through my graduate school.

TABLE OF CONTENTS

1. Introduction

1.1 Energy

The development of industry and daily lives of humanity heavily depends on the use of fossil fuels, and there are always concerns for their depletion. The shale gas revolution has introduced a new method for people to acquire oil and natural gas economically, but the utmost challenge with traditional energy sources is the environmental impacts associated with using them. According to NASA the average global temperature has increased by more than 1ºC since 1880. A widely-accepted hypothesis is that global warming is the result of the emission of CO_2 and other greenhouse gases into the atmosphere, which is mainly caused by using fossil fuels. Reduce the amount of CO_2 emitted into the atmosphere is a crucial step in alleviating global warming.

People have been searching for energy sources, which are both environmentally and economically applicable, to serve as feasible alternatives for the traditional energy sources. For instance, photovoltaic has been a hot research topic for the past several decades because of the possibility of converting the infinite solar energy into electricity. In practice the installation of solar panel can take a large space to reach optimum exposure to sunlight while the energy conversion efficiency of commercial solar panels is typically around 10~20%, which degrades over time and is much less than the efficiency of using fossil fuels. Unfortunately, it has been proven to be difficult to find new energy sources that are competitive to the traditional energy

sources in terms of energy efficiency and cost effectiveness. A variety of energy sources have been investigated, but many remain in the early stages of development.

1.2 Hydrogen

H_2 is a promising source of new energy because of its energy density, low emission, and the ability to be obtained from various sources [1], and it can be used in low emission transportation and power generation applications. However, H_2 is not naturally abundant, and the most likely route to acquire it is to convert from H_2O via electrical and chemical means. Due to the abundance of coal, large scale production of H_2 can be achieved through the reaction of coal and steam. The product of coal gasification is syngas, a mixture of H_2, H_2O, CO, H_2S and CO_2. Great interests have been invested the development of a cost-effective gas purification method, so that the H_2 can be utilized and the harmful gases can be processed and prevented from entering the atmosphere [2]. A variety of gas separation methods have been investigated, for example, cryogenic recovery, solvent adsorption, and membrane separation [3]. Among them, the most compelling method is to develop a gas separation membrane because of its low operating cost and low energy consumption [4].

1.3 Palladium based gas separation membrane

Pd was found to have high H_2 permeability and selectivity [5], and the most commonly used gas separation membranes are made from thin films of Pd or Pd based alloys. However, Pd is a costly metal and the surface of Pd is chemically unstable in sulphur containing gases, carbon containing gases, and steam. Since the demand for

Pd based separation membrane increases, the cost of Pd would only be driven higher. As a result, in recent years the focus of research has shifted from pure Pd to Pd based alloys which are relatively low cost and more chemically stable to syngas.

Shown in Fig. 1 is a schematic for a set of devices setup for gas permeation measurement, which represents a standard method to measure the H_2 permeability of a test membrane [9]. The test gas is applied at the feed side of the membrane at a certain pressure, and the vacuum is applied at the permeate side of the membrane. Pressure changes on the permeate side will be detected and recorded to calculate the hydrogen permeability of the test membrane. The basics idea behind the standard permeability method is to compare the difference in gas flow between the permeate and feed side of the membrane. A wide range of Pd binary alloys have been examined using this measurement method, but not much have been done to the ternary alloys. The binary alloy membranes used in this permeability test are prepared by placing the two metal membranes and provide heat to let them interdiffuse. At least one membrane per alloy component is required for sample preparation, which prohibits the fabrication of ternary or higher order alloys. The limitation in sample composition is one of the two major disadvantages in traditional permeability tests, the other disadvantage is obvious that only one material composition can be test per run.

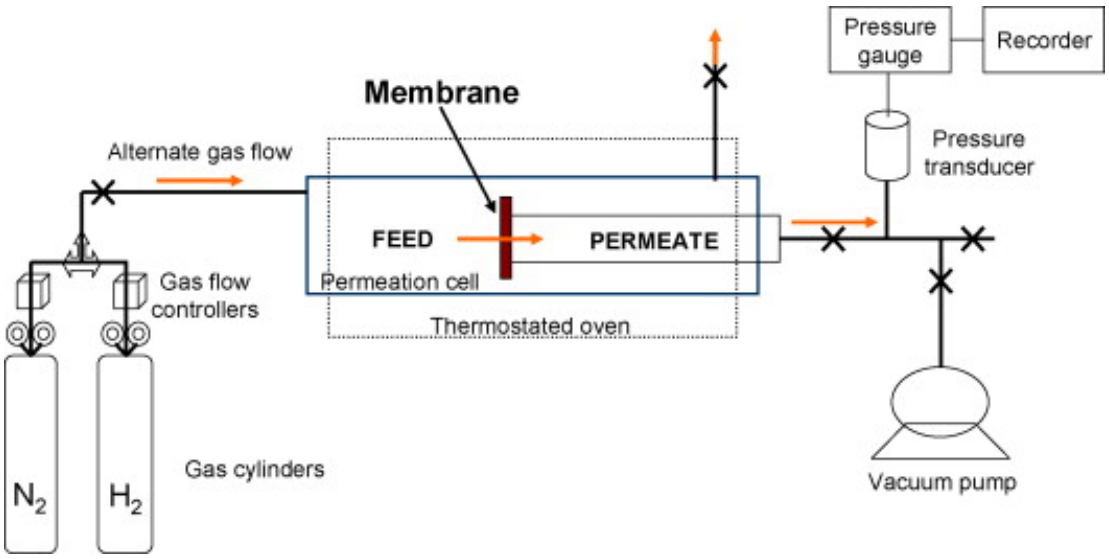

Fig. 1 A schematic that shows the equipment setup during a standard permeability test.

An alternative approach for measuring the hydrogen permeability was presented by de Man et al [7], a schematic of the alternative sample setup is shown in Fig. 2. In their method, the Pd alloy test material is deposited on a silicon substrate and an yttrium layer is deposited on top of the test material as hydrogen indicator. Some pure Pd dots are deposited on top of the indicator, and the Pd-free area are covered with yttrium oxide that serves as hydrogen barrier. During permeability test, H_2 molecules would dissociate into H atoms upon the contact with Pd dots. The H atoms would then diffuse down into the indicator layer, causing a color change, as well as migrate further down onto the test material. The lateral diffusion of H atoms in the test material would cause expansion in color changed area in the indicator, which can be measured and used in permeability calculation.

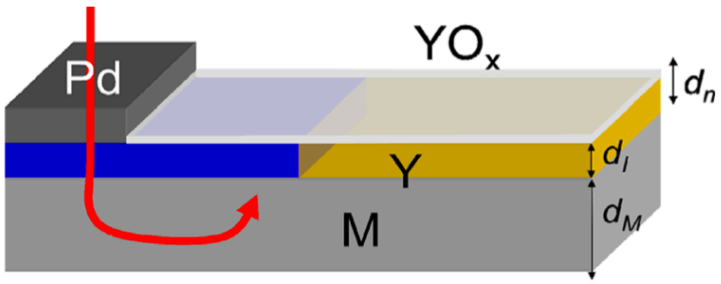

Fig. 2 A schematic of the alternative permeability measurement method presented by de Man et al.

The test material in the new sample setup is no longer bound to binary alloys since it is now prepared using deposition, and complicated composition spreads can be deposited and examined. The Pd dots at on the sample surface dissociates that H_2 molecules so the permeability of the test material underneath the dots can be visualized and calculated. Therefore, parallel examination of multiple compositions can be achieved by creating multiple Pd dots on the sample surface, which greatly improves the efficiency of permeability test. However, the disadvantages with this new method is also obvious. As discussed before Pd is chemically unstable in syngas, therefore this new method can be applied only without the presence of any harmful gases. Yttrium is chemically unstable in air, therefore when deposited at the surface of the sample it can be hard to work with. Overall, this new method inspired us to develop a competitive method that can be applied in the presence of C and S containing gases, while also allows parallel analysis of a multitude of Pd alloy compositions.

2. Method and Experiment setup

2.1 Sample setup and experiment procedure

The sample consists of three layers: a hydrogen barrier, the Pd alloy being tested, and a hydrogen indicator. The components are sputtered on a 3-inch glass wafer so that the hydrogen indicator can be observed. A schematic cross-section of the sample layers and a view of the film side of the sample are shown in Fig. 3. The Pd alloy test material is a composition spread with the species co-sputtered from up to 3 directions, the details will be discussed later. A total of 89 holes with 2mm diameter are opened in the hydrogen barrier. This setup allows designed areas of the test membrane to be exposed to the ambient gas while in direct contact with the indicator, and makes it possible for parallel evaluation of up to 89 different compositions.

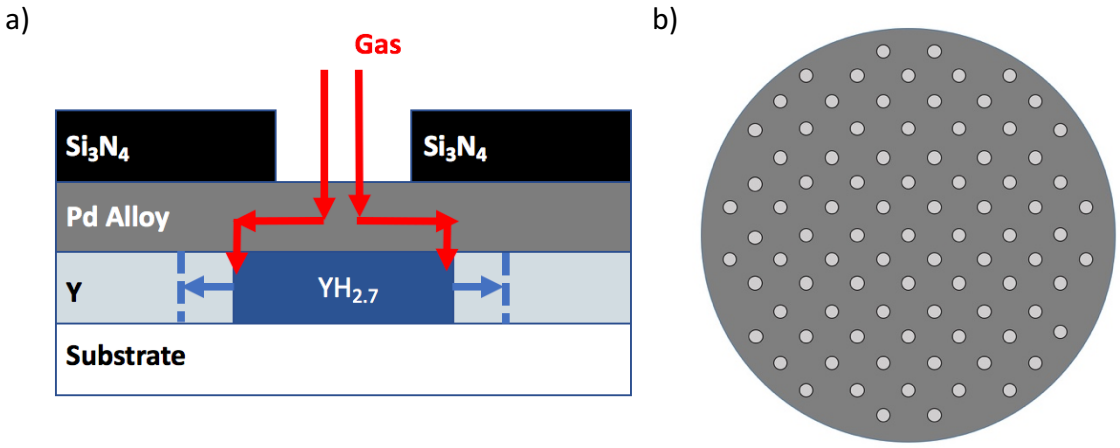

Fig. 3 (a) Cross-section of the sample layer. (b) Film side of sample with 89 holes patterned on the surface of nitride.

The hydrogen diffusion coefficient in Si_3N_4 is $1x10^{-19}$ cm^2/s under room temperature [8]. This makes it a good hydrogen barrier compared to Pd alloys because pure palladium has a hydrogen diffusion coefficient in the order of $1x10^{-7}$ cm^2/s under room

temperature. When the sample is exposed to hydrogen gas containing test gas, H_2 will only enter the Pd alloy under the area that is not covered with Si_3N_4. Upon contact with Pd alloy, H_2 dissociates into H atoms and diffuses through the test material into the indicator layer underneath, yttrium in our case. Y changes color from silver to blue when it forms the hydride ($YH_{2.7}$). It also acts as a hydrogen sink because the enthalpy of hydride formation is approximately -110 kJ/mol H in Y, much lower than -19.2kJ/mol H in Pd [7]. Since the H permeability in Pd alloys is orders of magnitude higher than that in Y, H atoms mostly migrate laterally within the Pd alloy and would then diffuse into the Y layer to cause an expansion in color changed area [7]. The growth in color changed area can be observed through glass substrate, and can be used to quantitatively determine the hydrogen permeability of the corresponding Pd alloy composition. Fig. 4 presents the standard experimental procedure used in this project, and the detail of each step will be discussed later.

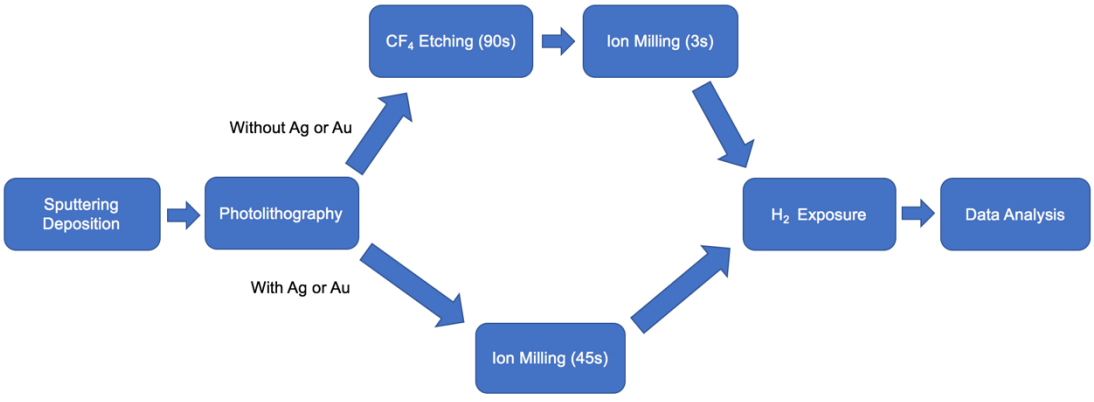

Fig. 4 Standard experimental procedure.

2.2 Sputtering deposition

The thin films are deposited in a custom-built DC magnetron sputtering chamber, which was designed for depositing composition spread thin films. The chamber is capable of depositing three 3-in diameter substrates in one pumpdown, and it has an array of four-magnetron sputtering guns. A schematic of the gun arrangement is shown in Fig. 5. A uniform under layer can be sputtered from the center gun, while the side guns are located at the vertices of an equilateral triangle and allow simultaneous deposition of up to three species. There is another large 4-in diameter DC magnetron gun in the chamber, that allows the deposition of uniform diffusion barrier layer. The sputtering rate of each individual gun or the overall rate during co-sputtering can be measured using a water-chilled quartz crystal thin film thickness monitor (XTM).

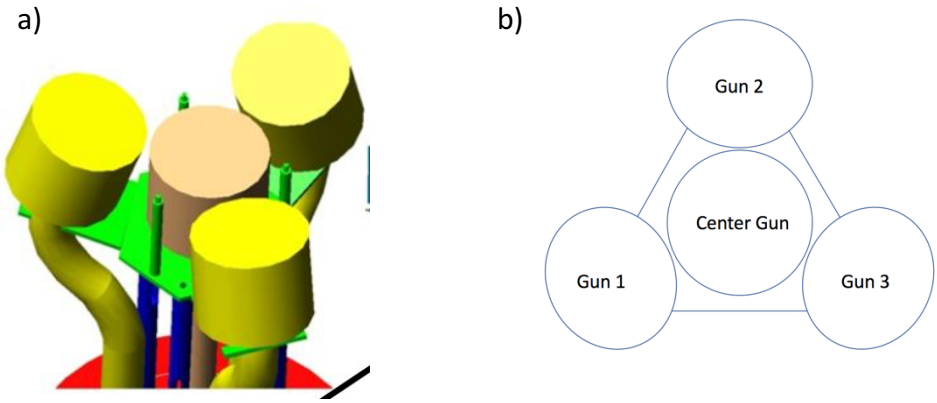

Fig. 5 (a) Schematic of the 4-gun cluster in the deposition chamber. (b) The orientation of each sputtering gun with respect to the substrate, same for the later schematics.

The system uses a mechanical pump for rough pumping, and as well a cryopump for pumping the chamber to high-vacuum regime. The typical base pressure is around $3x10^{-7}$ Torr. The system can use four gases for sputtering: Ar, N_2, CH_4, and O_2, to make a variety of materials. For this project, Ar is used as the basic working gas and

N_2 is used in reactive sputtering of Si_3N_4. The gas flow rate is typically set to 75 standard cubic centimeters per minute, and the sputtering pressure is typically between 0.6~1 Pa. For a 3-in diameter substrate, the relative deposition rate of the three side guns is approximated using the equation:

$$d = -1.42 + 1.037 * \left\{1 + \left[\frac{(x - 47.7)}{42.96}\right]^2 + \left[\frac{y - 0.41}{67.7}\right]^2\right\}^{-1} \qquad \textit{Eq. 1}$$

where d is the relative deposition rate, x and y are the coordinates with the origin being the center of the substrate (Fig. 6). This is an empirical fit to measured thickness profiles of typical thin films deposited from the side gun in this system. The XTM is only set to measure the deposition rate at the center of substrate. With the fitting equation one can calculate the actual sputtering rate over the whole substrate for each element being co-sputtered, thus calculate the thickness and composition at any specific location.

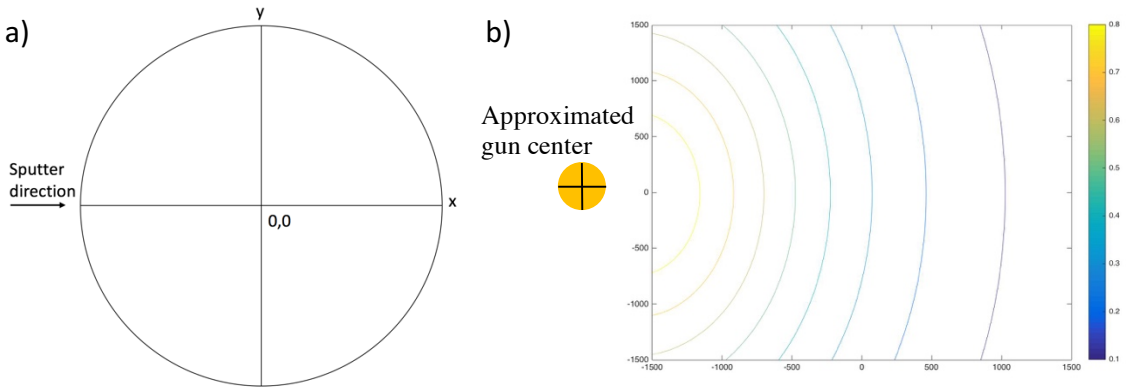

Fig. 6 (a) Schematic of the substrate with the coordinate system used for rate calculation. (b) Contour of the relative deposition rate for material deposited from the approximated gun center.

2.3 Sample processing

Samples are patterned at Cornell NanoScale Facility(CNF) using photolithography and etching. The samples are cleaned with isopropyl, primed by spin coating with hexamethyldisilazane, and finally spin coated with Shipley 1813 photoresist using a spin coater. The resist film has an approximate thickness of 1.3μm and is baked at 115˚C for 60 seconds. After exposure using a Suss MA6-BA6 contact aligner for 10 seconds and developing using Hamatech-Steag wafer processor with AZ 300 MIF developer, the samples are dry etched with CF_4 for 90 seconds in Oxford 81 dry etcher. The photoresist is removed using acetone and isopropyl alcohol, and the samples are etched in AJA ion mill for 3 seconds to remove any residual surface contamination that could could hydrogen diffusion or dissociation. Samples containing gold and silver are not allowed in the Oxford 81 because they might contaminate the chamber. These samples are etched using the AJA ion mill for 45 seconds directly after being exposed, in which case no additional ion milling is required after the removal of photoresist.

2.4 Exposure

A custom-built tube furnace is used for hydrogen exposure of processed samples, as is shown in Fig. 7. The major component of this tube furnace is a 4-inch diameter quartz tube that is sealed at both ends. Gas bubblers are attached to each end of the quartz tube to allow excess gas to escape from the chamber, maintaining a small positive pressure and prevent any back flow. Test gas flows through a rotameter and directly into the tube. A diffuser made from aluminum mesh and quartz wool is used to create

a uniform gas flow in the tube. An ATS furnace controller is used to power the Watlow ceramic heater located at near the center of the tube furnace to obtain the desired temperature. However, in this project all the experiments are done at room temperature. During exposure, the sample is inserted glass side up inside the furnace, which allows real time visualization of color change and dot expansion. After certain amount of time (typically 5 hours), the exposed sample is withdrawn from the tube and a photo of the indicator side of the sample is taken for dot size analysis.

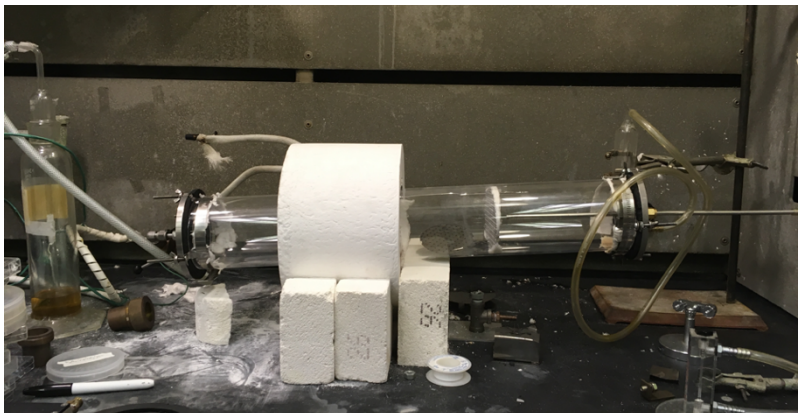

Fig. 7 Setup of the tube furnance.

2.5 Experiment photos

2.5.1 Photo taking and photo processing

The reflective indicator on the glass substrate makes the indicator side of the substrate a mirror. Taking the substrate photo directly above the indicator side gives an image of the camera and no dots could be observed. This problem was solved by taking the photo at an angle inside a light box, the system setup is shown in Fig. 8. The light box provides diffuse white light, which gives good contrast between the silvery background and blue dots. The camera is set at an angle so the sample only reflects the

white plastic sheet of the light box. A grid paper was placed beneath the sample to provide a scale for dot size measurement.

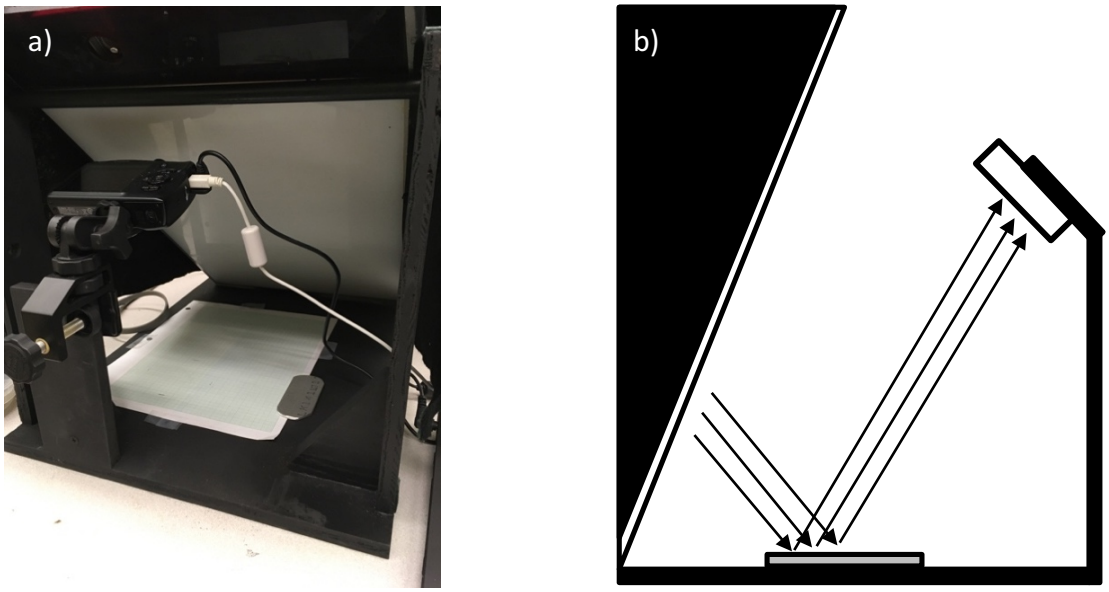

Fig. 8 (a)Setup of the camera inside the light box. (b) Schematic of the side view of the camera box

Our camera setup solved the problem of mirror reflection sample, but introduced new problems into the photos taken due to the height and angle of the camera. One of the problems is foreshortening distortion: a 1cm grid line close to the camera is generally 10% longer than a 1cm grid line located further away in terms of the number of pixels. This problem would affect the radii calculated using Hough transformation because the actual length represented by 1 pixel varies across the sample. The result is that the calculated radii of the dots located at the bottom part of the sample would be greater than the dots located at the top part. Another often observed problem is radial distortion, in which one would find the straight grid lines curved inward (pincushion distortion) or outward (barrel distortion) in the image. The barrel distortion causes the shape of the substrate in photo changes from a perfect circle to an irregular shape, which further affects the shape of the dots on the sample. Because Hough

transformation only detects shapes that are close to a circle, the change in dot shape would influence the result of dot detection, radii calculation and eventually permeability calculation.

Adobe Photoshop was used to correct the distortions. The radial distortions were corrected using the "lens correction" function, which "squeezes" or "stretches" the image to remove the curvature. The grid lines in the image were aligned using the "free transformation" function, and the Photoshop built-in grid was chosen to be the reference. Adjustments were performed on the image to transform the substrate into a perfect circle. Artifacts on the substrate, like writings, were removed to improve the accuracy of Hough transformation. The image was cropped to focus on the substrate. On the processed image, the length difference between a 1cm grid line close to the camera and a 1cm grid line furthest away from the camera is reduced to less than 1%, which is not significant relative to the resolution of radii and permeability calculation. Fig. 9 shows the comparison between the original image and the processed image of the same sample.

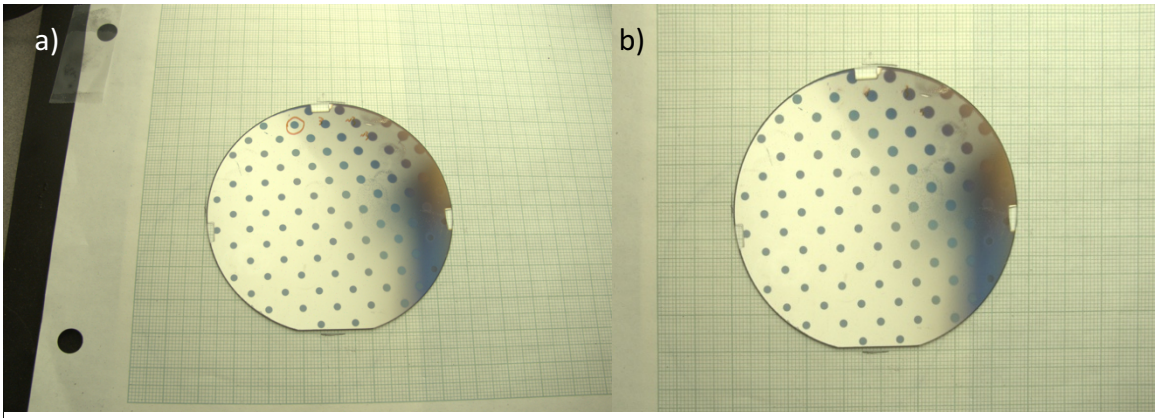

Fig. 9 (a) Original photo, from which severe distortion can be observed. (b) Processed image, in which majority of the distortion have been removed.

2.5.2 Transforming photo to get calibrated Cartesian coordinates

The photo of each sample after exposure to H_2 gas are analyzed using Matlab to measure the size of each dot. Our objective is to calculate the permeability of the dots based on their radii, and search for the trend of how permeability varies with the composition of Pd based test material. The thickness at each dot is necessary to calculate the composition and permeability of the corresponding test material. As discussed in section 2.2, the relative deposition rate of a target located in the x direction is approximated using equation 1, with the origin set to be the center of the substrate. In practice the three offset guns of the 4-gun cluster are located 120 degrees away from each other, but none of them are in the x direction. The axis of equation must be rotated 210 degrees counterclockwise, 90 degrees counterclockwise, and 30 degrees clockwise to align with the position of gun 1, gun 2, and gun 3 respectively. This adjustment in coordinate system allows us to properly simulate the thickness gradient of the materials deposited from three different directions, and calculate the corresponding alloy composition and hydrogen permeability.

2.6 Hough transformation

The substrate photo is converted into grey scale before the analysis, so that the color changed regions appear as darker pixels and the background appear as brighter pixels. Dot size analysis is carried out using the Matlab built-in function “imfindcircles”, which is uses Circular Hough Transformation (CHT) to find circles in images and determine the radii of the circles found. The algorithm scans across the loaded image

and detects every dark pixel. For each dark pixel detected, circles of all possible radii are created with that pixel being the center.

$$(x-a)^2+(y-b)^2=r^2 \qquad Eq.\ 2$$

The created circles would intersect with each other, and the variable a's and b's that has the maxim local intensity are determined to be the actual centers of the blue dots while the radii that gives the highest intensity is determined to be the actual radii of the blue dots. Usually there are more than 60,000,000 pixels in one picture, and the transformation typically takes about 20 seconds on a 2013 Macbook Pro.

2.7 Permeability Calculation

The permeability calculation of Pd alloy is carried out using Matlab. Hough transformation can locate the centers of each blue dot on the indicator side, and could also calculate the radius of each found dot. As described by de Man [7], the permeability associated with a blue dot is calculated using the following equation:

$$k=\frac{1}{8}\frac{c_I d_I}{d_M\sqrt{p}}R^2\left\{\frac{2\left(\frac{r_f}{R}\right)^2\left[\ln\left(\frac{r_f}{R}\right)-\frac{1}{2}\right]+1}{t}\right\} \qquad Eq.\ 3$$

where k is the permeability (mol/m/s/$Pa^{0.5}$), c_I is the hydrogen concentration in yttrium (mol/cm^3), d_I is the thickness of yttrium layer (A), d_M is the thickness of catalyst layer (A), p is the hydrogen pressure (Pa), R is the radius of palladium dot (mm), r_f is the radius of color changed dot (mm), and t is the exposure time (s). A schematic is shown in Fig. 10. The standard value for R is 1mm, which is the radius of a Pd dot; the value for p is 500 Pa because the exposure is performed at 1atm with 5% H_2 gas; The

hydrogen concentration in $YH_{2.7}$ is reported to be 1.8mol/cm^3 [], which is used as the standard value of c_I.

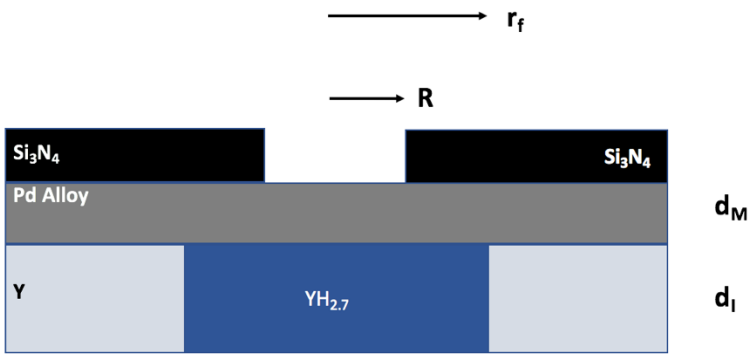

Fig. 10 Schematic of the cross-section of the sample underneath exposed test material. Note that the thickness of the layers not to scale.

3. Results and Analysis

3.1 Method development

This high throughput method for hydrogen permeability analysis follows on the research initially conducted by Christopher Mizzi [10]. Many adjustments have been done to make it work successfully.

3.1.1 Indicator selection

Tungsten oxide ($WO_{3)}$ was originally used as the hydrogen indicator by Mizzi. WO_3 forms a tungsten bronze when it absorbs hydrogen ($HxWO_3$, $x<0.6$), and changes color from brown to blue [11]. WO_3 could also act as a hydrogen sink: it has low hydride formation enthalpy (-30kJ/mol H) comparing to the hydride formation enthalpy of Pd (-19.2kJ/mol H) [7]. In practice, WO_3 changes color and the color changed area expands under hydrogen exposure, which indicates that WO_3 has higher hydrogen diffusivity comparing to Pd. However, the color changed area shrinks and quickly disappears quickly after the sample is removed from hydrogen source. Our hypothesis is that the difference in hydride formation enthalpy is not large enough for hydrogen to be permanently trapped in WO_3 as hydride. Instead, for low hydrogen pressure (room air), hydrogen atoms diffuse back into Pd and recombine into H_2 at Pd surface. To be a good indicator, the material needs to change color quickly after absorbing hydrogen atoms, and the color changed area needs to be sufficiently permanent to allow analysis. We replaced WO_3 with Y for this reason, and found that Y works outstandingly as the indicator.

3.1.2 Etching method

In the original method, samples are etched with CF_4 for 90 seconds to remove the Si_3N_4 under areas exposed during photolithography, followed by a 30 second O_2 etch to remove any residual organic material on the surface. Problems were observed after the samples were exposed to H_2 gas. One sample which has 25nm of Y, 40nm of Pd, and 50 nm of Si_3N_4 (center thickness of each layer) was exposed for 12 hours in 5% H_2 gas, and the picture of which is shown in Fig. 11. Note that H_2 gas was pointed directly onto the Pd surface before the nitride was deposited to test if the Pd and Y were functional. Y changed color instantly when H_2 gas contacts the Pd surface, and results in a large blue dot. This experiment shows that pure Pd dissociates H2 instantly and the indicator works as expected.

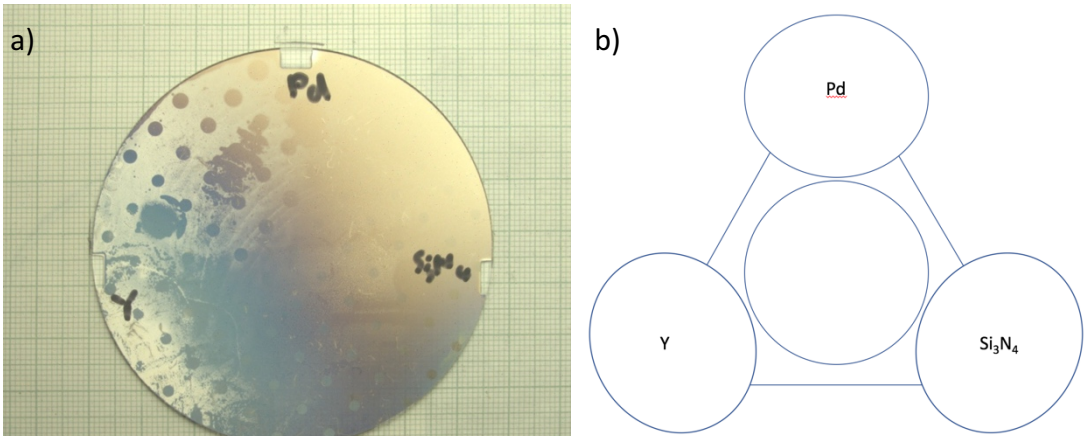

Fig. 11 (a) Indicator side of a pure Pd sample exposed in 5% H_2 gas for 12 hours. Majority of the substrate changed color, but the large blue dot is the result of Pd testing before the nitride was put down. (b) Setup sputter guns in the 4-gun cluster.

After the exposure, few dots are observed while a large fraction of the indicator changed color even in regions covered with Si_3N_4.Y was deposited from gun 1, and

the thickness of the Y layer decreases as it moves away from the bottom left part of the substrate. Thinner Y takes less H atoms to form hydride and change color, which means lower resistance to long term exposure to H_2 gas. Another possibility is that the etching method was not sufficient to expose the Pd dots, so it takes too long for the hydrogen diffuse through them—longer than the Si_3N_4 can hold.

To isolate the effect of etching, a substrate was sputtered (30nm Y, 55nm Pd, and 75nm Si_3N_4 at the center) and cut into 8 pieces for different lithographic patterning and etching processes (Fig. 12). During deposition half of the substrate was covered with aluminum foil (piece 2, 3, 4, and 5 in figure) to prevent Si_3N_4 from depositing that part of the substrate. The etching processes used and the observations after 8-hour exposure to H_2 at room temperature are included in Table 1.

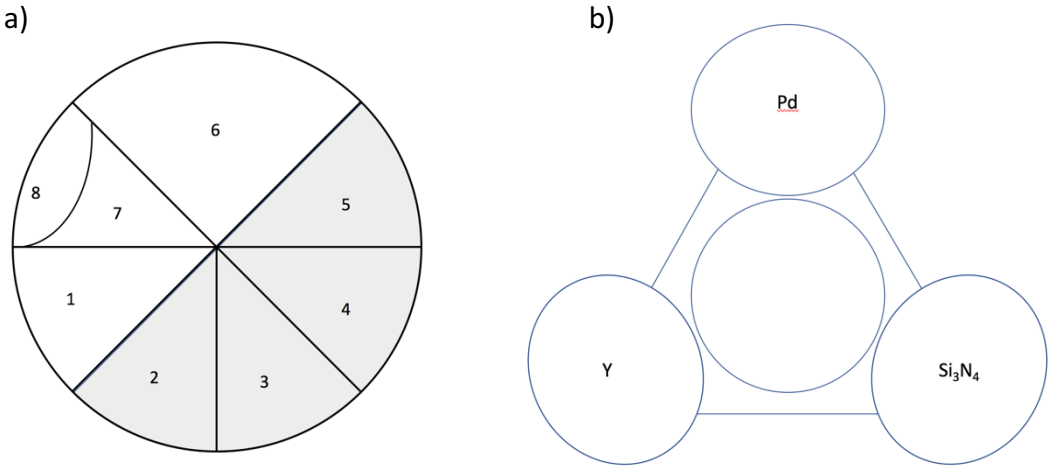

Fig. 12 (a) The sample was broken into 8 pieces to investigate the effect of etching process. The white pieces were covered with Al foil during nitride deposition while the grey pieces were not covered with Al foil. (b) Setup of the sputter guns in the 4-gun cluster

Pieces	Processing Method	Observations
1, not covered with Al foil	Patterned with lithography, CF4 etch, O2 etch	No color change
2, covered with Al foil	Nothing	No color change
3, covered with Al foil	CF4 etch	Color change
4, covered with Al foil	CF4 etch, O2 etch	No color change
5, covered with Al foil	Nothing	No color change
6, not covered with Al foil	Nothing	No color change
7, not covered with Al foil	CF4 etch, O2 etch	No color change
8, not covered with Al foil	Patterned with lithography, CF4 etch, O2 etch	No color change

Table 1 Treatment during deposition, etching method, and observation after 8 hours of exposure to 5% H_2 gas for each piece of the pure Pd sample.

Pieces 7 and 8 were covered with Si_3N_4, but they failed to change color after being etched with CF_4 and O_2. Our hypothesis to explain this observation is that the O_2 etch may contaminate the sample surface and prevent hydrogen dissociation. Strangely piece 2, 4, and 5 also had no color change even though they should have no Si_3N_4 on them at all. Fig. 13 shows the photo of pieces 2, 3, and 4 after 20 hours of exposure to H_2. Among them piece 3 is the only one that changed color. We hypostasized that some Si_3N_4 was unintentionally deposited on the Pd surface (the Al foil was not tightly secured against the sample), and that the combination of CF_4 and O_2 etch failed to remove the nitride.

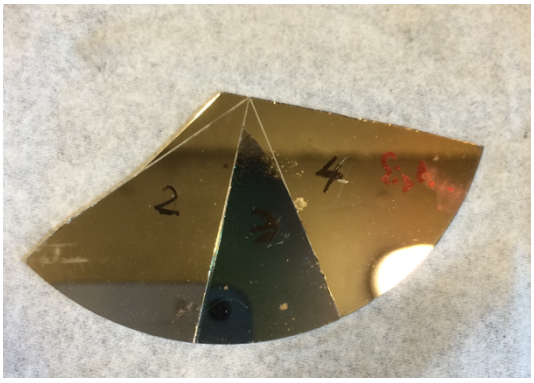

Fig. 13 Piece 2, 3, and 4 after 20 more hours of exposure.

To further understand whether O_2 etch is necessary, pieces 2, 4, and 5 were etched again with CF_4 for 90 seconds. Piece 6 was patterned using photolithography and etched with CF_4 for 90 seconds. All the pieces were then exposed in 5% H_2 gas for 20 hours, an image was taken and shown as Fig. 14. Dots appeared under exposed Pd on piece 6, while piece 2, 4, and 5 all changed color. Although there is no evidence suggesting that O_2 etch contaminate the surface of test material, it is proven that the CF_4 etch alone is sufficient to remove the nitride and expose the test material. Thus, O_2 etch was removed from the etching procedure.

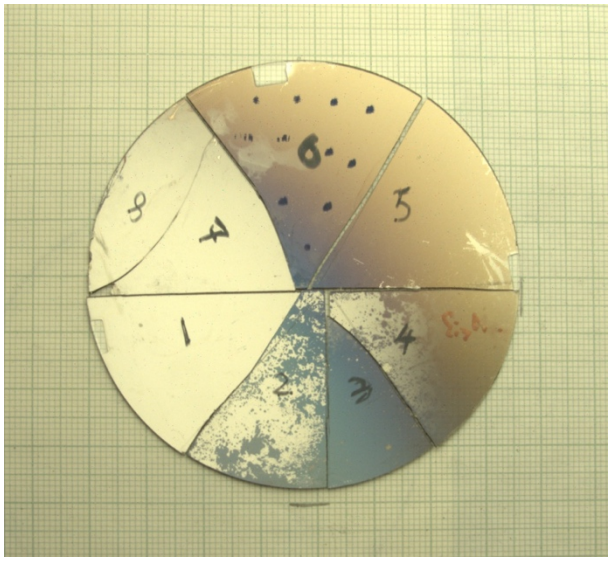

Fig. 14 An image of all the pieces exposed in H_2 gas for 20 hours. Dots appeared on piece 6, while piece 2, 4, and 5 all changed after CF_4 etching.

Fig. 15 shows a sample (80nm Y, 50nm Pd, and 65nm Si_3N_4 at the center) that has been etched with CF_4 alone. After exposure in 5% H_2 in Ar for 15 hours, some dots did not appear on the indicator. The previous experiment demonstrated that for pure Pd on Y (with no Si_3N_4), the indicator changes color instantly upon exposure to H_2. Therefore, we concluded that for this pure Pd sample there must be some unknown contaminants on the exposed Pd dots, which prevents the hydrogen dissociation. We introduced a 3-second ion milling step into sample processing to remove any surface contamination remaining on the Si_3N_4 openings. Ion milling is done with pure Ar, so it should not introduce any surface contamination, though it might introduce disorder.

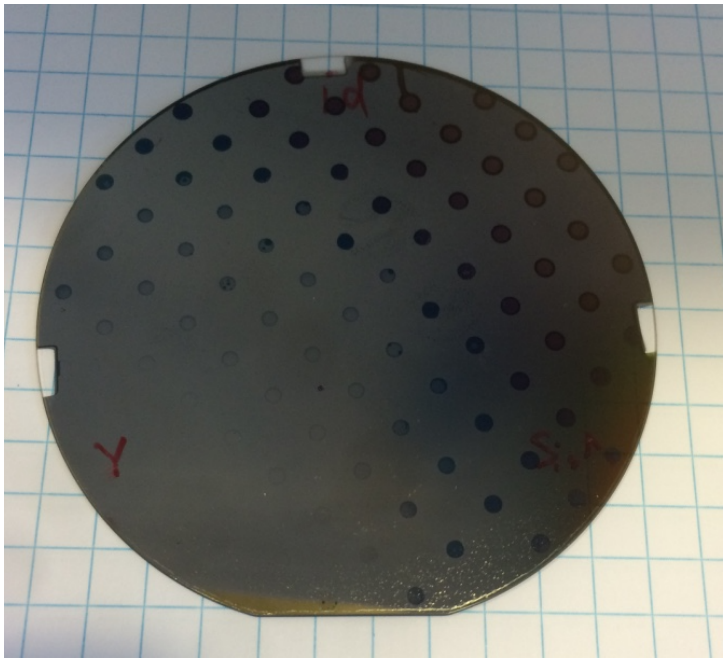

Fig. 15 An image of pure Pd on Y after 15 hours of exposure in H_2 gas.

Shown in Fig. 16 is a sample that has been prepared identically as the one shown in Fig. 15. But, as a last steip, etched with the ion mill for 3 seconds. Note that in Fig. 16(a), the blue dots inside the red box appeared instantly when a tube with flowing H_2 gas was directed toward the exposed Pd. After 3 hours of exposure to uniform 5% H_2 gas in the tube furnace, a photo was taken and shown in Fig. 16(b). It can be observed that all the dots appeared as expected, except in the lower right where the nitride was apparently not completely removed. This set of experiments proved that the removal of the several layers of atoms on the surface of thin film after lithographic processing did remove some contamination that effectively blocks the hydrogen dissociation and diffusion. This step was a critical improvement in the experimental procedure.

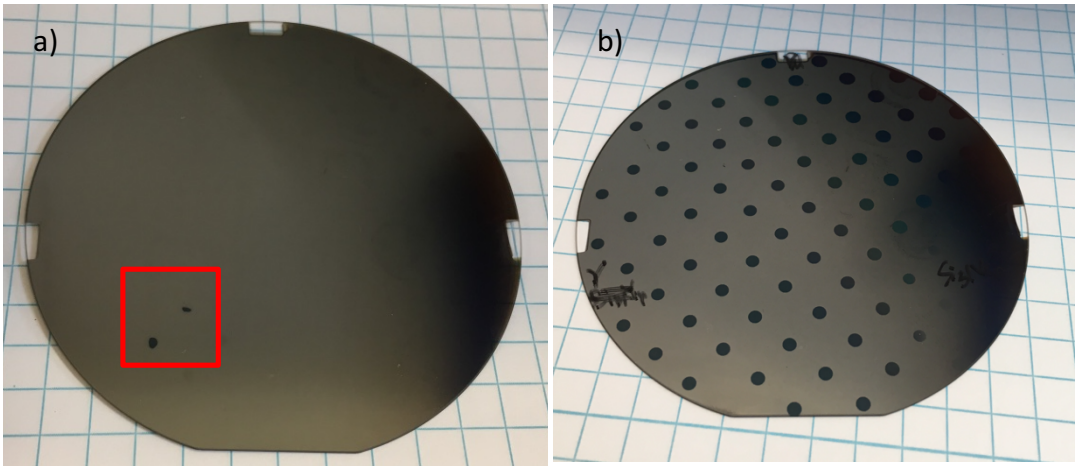

Fig. 16 Image of the substrate prepared identically as the one shown in figure 12, with the addition of ion mill etching as the last step. (a) Two blue dots appeared instantly when the exposed Pd contacted H_2 gas. (b) Almost all the dots appeared on the indicator after 3 hours or exposure to 5% H_2.

3.1.3 Parameters for nitride deposition

A set of experiments are conducted to investigate how the sputtering parameters of nitride influences its hydrogen blocking ability. 80nm of Y and 55nm of Pd (at the center of the substrate) was deposited on a 3-inch glass substrate, which was then broken into 3 pieces. The middle piece was kept as a control while the other two pieces were each broken into 3 smaller pieces to test different nitride deposition conditions. Typically, the nitrides were deposited at 7.5mTorr with 13% N_2. In this set of experiment the nitrides were deposited from the 4-inch gun at 7.5mTorr, 9mTorr, and 12mTorr with 13% N_2. The thicknesses of the nitride layers were designed to be 28nm and 35nm. Fig. 17 shows the deposition condition and thickness of the nitride deposited on each piece, note that piece 5 has only about 23nm of nitride due to timing error during deposition. After exposure to 5% H_2 gas for 5 hours, the nitrides deposited at 9mTorr and 12mTorr stopped H_2 from diffusion through. The only piece that changed color was piece 4, which was deposited at 7.5mTorr and has a thin nitride thickness. We concluded that the thickness is the only significant contributor to the nitride's hydrogen-blocking ability because piece 3, which was deposited at 7.5mTorr but has a thicker nitride, worked well blocking hydrogen in 5 hours.

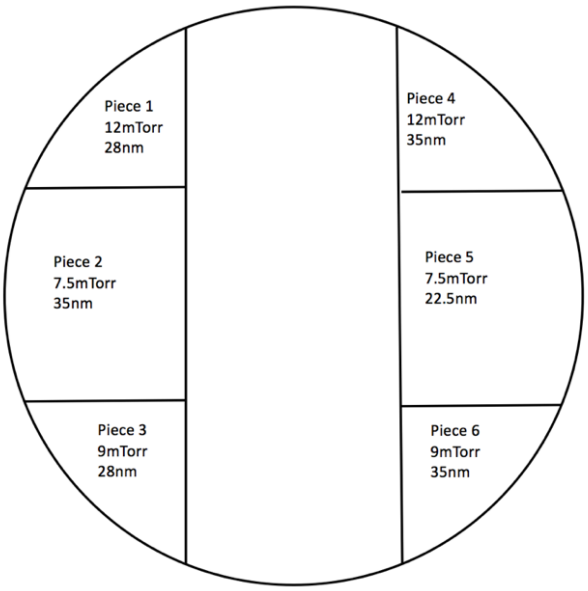

Fig. 17 Deposition condition and the thickness of the nitride layer deposited on each piece of the pure Pd sample. Only piece 5 changed color after 5 hours of exposure to 5% H_2 gas.

Three fragments were broken from the center piece that was nitride free, and were deposited with 45nm, 55nm, and 65nm nitride at 7.5mTorr respectively. The preparation for all the pieces is shown in Fig. 18(a), note that piece 8 was patterned and etched before exposure. The three new pieces were exposed to 5% H_2 gas for 5 hours, and a photo of the whole substrate was take and shown in Fig. 18(b). The large blue dots appeared on the indicator served to check the catalysis ability of Pd, and provide a reference for color change. Piece 7 and 9 processed no color change after 5 hours of the exposure, while dots under exposed Pd changed color on piece 8. The results showed that the nitride deposited at 7.5mTorr with a thickness higher than 23nm blocks hydrogen from contacting the test material for a reasonable amount of time. A nitride thickness of 55nm was used for all future sample as the hydrogen barrier.

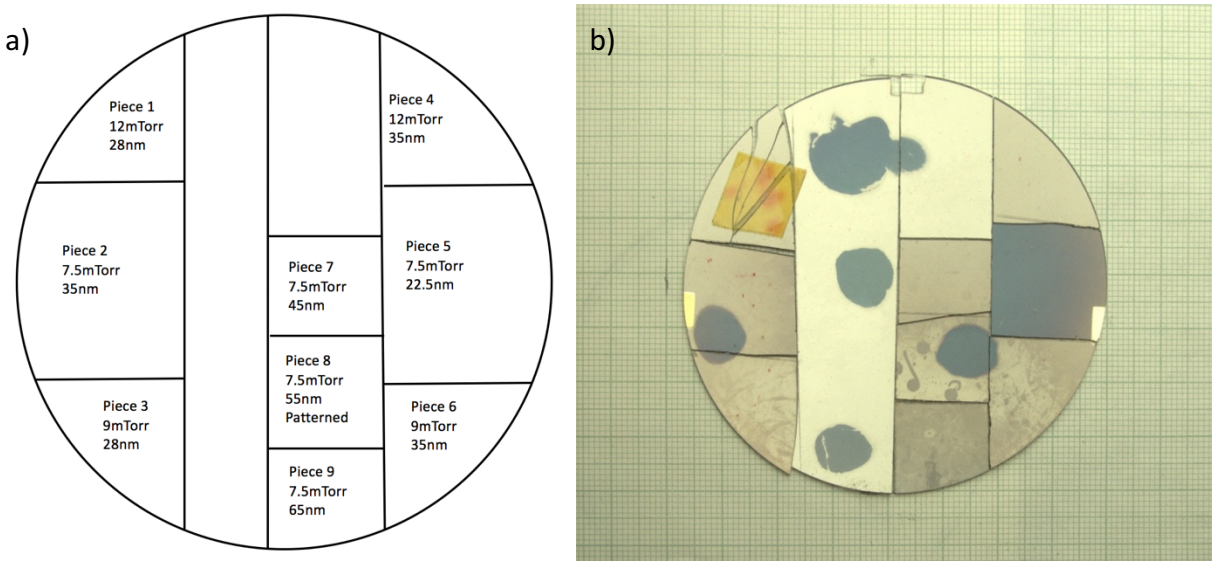

Fig. 18 (a)Deposition condition and the thickness of the nitride deposited on each piece of the pure Pd sample. Note Piece 8 was patterned before exposure to H_2 gas. (b) Image of the whole substrate used in the nitride testing.

3.1.4 Exposure method

In the original design samples are loaded in a movable semi-closed sample holder, which is connected to a ¼ inch diameter stainless steel tube, for hydrogen exposure (Fig. 19). Hydrogen gas flow through thin tube directly onto the film side of the substrate, and the compact volume of this substrate holder allows rapid change of gas environment around the sample. This setup is useful for permeability test at elevated temperature because the diffusion of hydrogen inside the test material would be much faster comparing to the diffusion at room temperature. Hydrogen gas would be introduced to the substrate when the tube furnace reaches desired temperature; hydrogen gas is switched off once the permeability test is finished, and the substrate holder is quickly pulled away from the heat source.

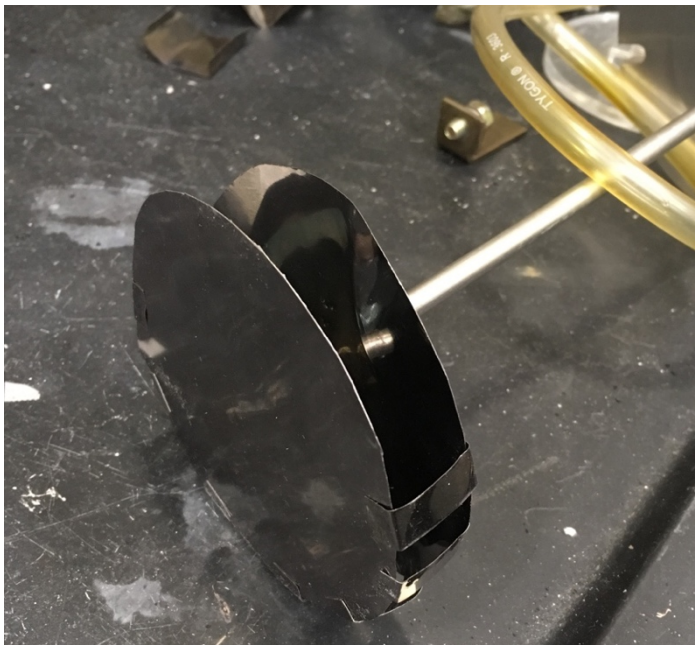

Fig. 19 A photo of the substrate holder used in sample exposure. The sample is loaded in the small chamber, with the film side facing towards the gas tube from which the H_2 gas enter.

In practice a problem arises from using the substrate holder. Shown in figure 20(a) is a pure Pd sample exposed for 8 hours using the substrate holder. All the dots have appeared yet many are hard to observe because more than half of the indicator changed color even under the nitride cover. The same problem was observed from multiple samples that were exposed using the sample holder. Our hypothesis is that the substrate holder is a compact structure and the sample surface close to the gas tube. Hydrogen gas was directed to blow at the center of sample surface and created a high local hydrogen concentration. The silvery area on Fig. 20(a) shows that the nitride had no problem blocking the hydrogen gas under normal concentration, but failed when the hydrogen concentration is high. Since we are not doing any experiments at elevated temperature, all future exposures were performed without the sample holder.

The substrates were loaded directly into the glass furnace, and a gas diffuser was constructed to further even out gas flow (Fig.20(b)).

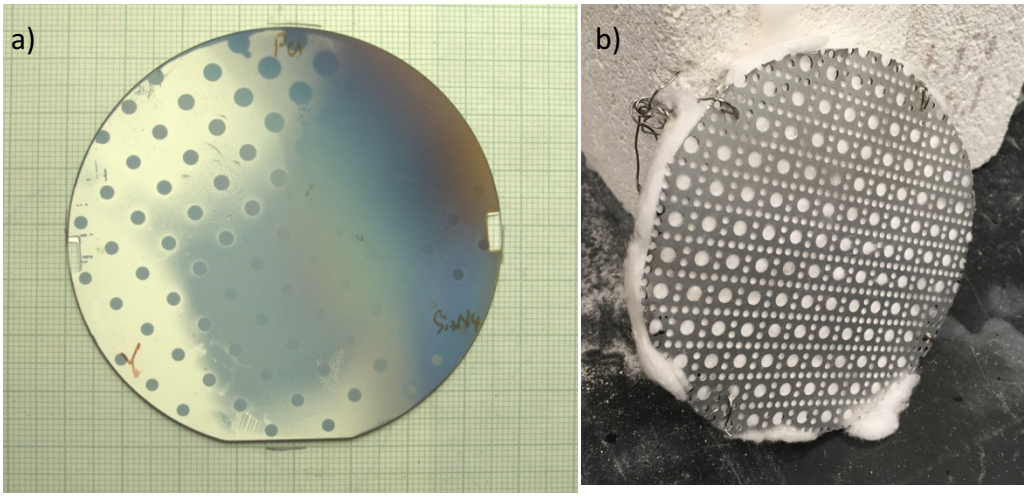

Fig. 20 (a) An image of pure Pd sample exposed in 5% H_2 gas for 8 hours using the substrate holder. (b) Photo of the self-made gas diffuser.

3.2 Actual samples, processing parameter, data analysis

3.2.1 Pure palladium

3.2.1.1 Gradient Pd on gradient Y

To check the validity of the sample design and Hough transformation, a sample was made with pure Pd being the test material (Pd sample 1). Y was deposited from gun 1 of the 4-gun cluster (80nm at the center), Pd was deposited from gun 2 (50nm at the center), and the nitride was deposited from gun 3 (65nm at the center). There is a gradient in all three layers because the species were all deposited from the side guns. The nitride layer was patterned using photolithography, etched with CF_4 for 90 seconds, and further etched in ion mill for 3 seconds. The sample was then exposed to 5% H_2 gas for 3 hours, and a photo of the indicator was taken for data analysis. The photo of Pd sample 1 was processed as shown in Fig. 21. A fraction on the right of the substrate changed color despite under the cover of nitride, and the dots appeared in that part are hard to see. This sample was exposed before we introduced the gas diffuser into the tube furnace, therefore during exposure the H_2 gas was directly hitting the substrate from the right. As a result, the H_2 concentration at the right of the substrate might be higher than that at the left, which makes it harder for the nitride to block the diffusion of hydrogen completely.

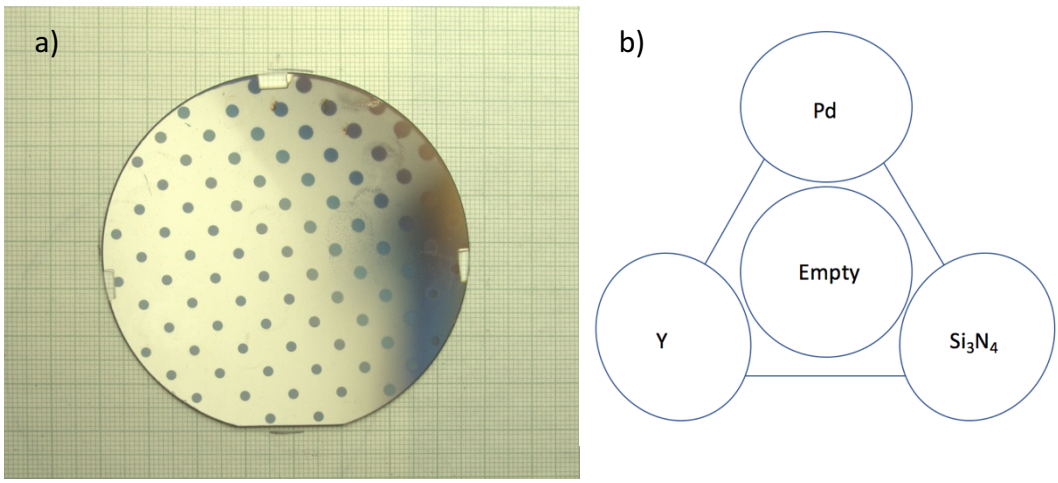

Fig. 21 (a) Pure Pd sample 1 after exposure to 5% H_2 gas for 3 hours. (b) Setup of the sputter guns of the 4-gun cluster

Hough transformation was performed on the processed image to find the centers of dots and measure the radii of the identified dots. A 1cm grid line was chosen to be the calibration for dot size measurement, and the center of the substrate was determined for deposition rate calculation. Fig. 22(a) shows the Hough transformation results for Pd sample 1, in which the red circles represent the dots detected and the numbers in the blue text boxes next to the Hough circles are the radii in millimeters. Most dots have been detected, except those that have irregular shapes or have poor contrast with the background. Part of the Fig. 22(a) is blown up and shown in Fig. 22(b) to give a closer look at the Hough circles around the dots. The Hough circle fits the periphery of the dot well, thus the Hough radius should give a precise estimate on dot size. The radius measurement is basically counting pixels that have brightness less than a certain grey value from the center of the dots. We improved the accuracy of measurement by allowing sub-pixel counting in our algorithm so that small variation in dot size can be measured.

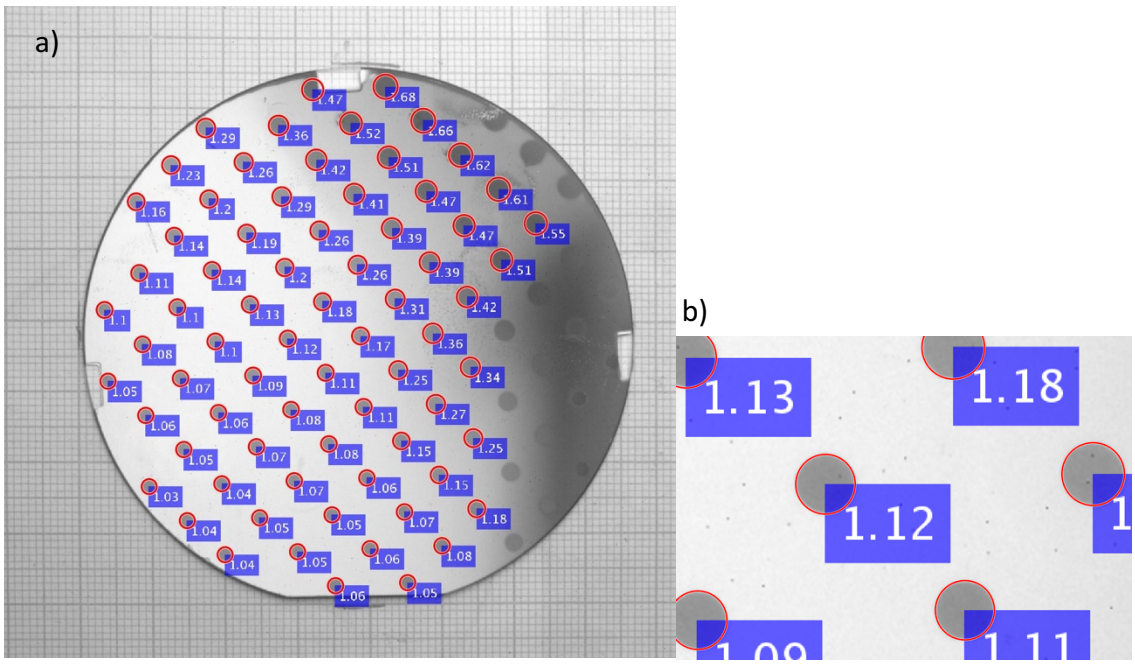

Fig. 22 (a) Result for Hough transformation performed on the pure Pd sample 1. (b) A fraction of the substrate was blown up to show the fitting of Hough circles to the actual dots.

To validate the Hough transformation analysis, some dots were measured using ImageJ. A line was drawn across the center of a dot and the brightness of pixels along the line were plotted against the length of the line. An example is shown in Fig. 23, the brightness of the pixels is constant on the dot and gradually increases towards the peripheral of the dot. The diameter of the dot is typically picked at the middle of the two curves. Each dot is measured multiple times and the average is taken to be the actual diameter of the dot. The dot measured in Fig. 23 is the same dot appeared in the center figure 22(b), which has Hough radius of 1.12mm. The radius of that dot measured using ImageJ was 1.13cm. This difference in dot size is not significant in permeability calculation using equation 3, thus proves the validity of Hough transformation.

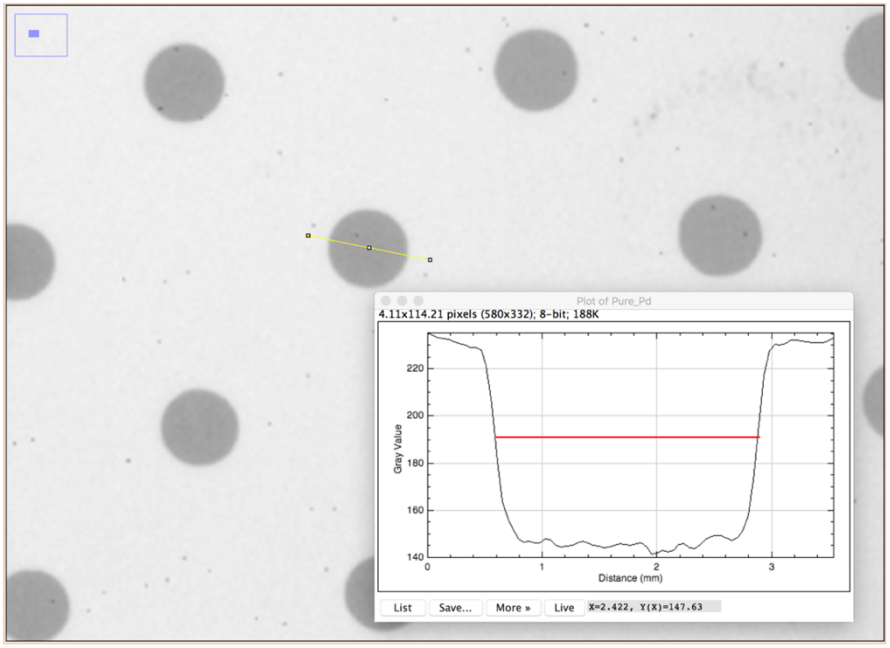

Fig. 23 Dot size measurement using ImageJ

As stated in the experiment setup section, the relative deposition rate from the side gun is approximated using Equation 1. During deposition, the actual deposition rate at the center of the substrate was measured using the XTM and is used as the reference to calculate the actual deposition rates across the whole substrate. The layers are deposited from different directions, and the coordinate system used in equation 1 is rotated to accommodate the changes. The thickness of each layer was calculated from the deposition rate and deposition time. Figure 22 shows the Pd thickness in Pd sample 1, in which a brighter color represents a higher thickness. Although the thickness of indicator layer was non-uniform, one could find from Fig. 22(a) and Fig. 24 that larger dots appear under thicker Pd. This result meets our expectation that thicker Pd has higher hydrogen permeance, so the dots would expand faster under thicker Pd.

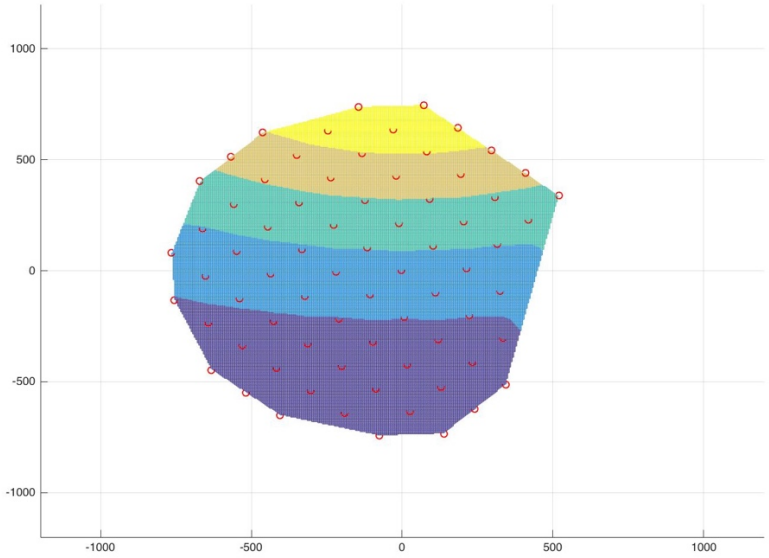

Fig. 24 The thickness gradient of the Pd layer on Pd sample 1.

The permeability of each dot is calculated using Equation 2. The permeability value is reported in units of $1x10^{-9}$mol/m/s/$Pa^{0.5}$ in Fig. 25 and the permeability mapping is shown in Fig. 26, where a brighter color represents higher hydrogen permeability. The permeability decreases as the Pd thickness decreases and Y thickness increases, but the permeability is the highest around the area where H_2 diffused through the nitride barrier. In the area where H_2 diffused through the nitride, there is less contrast between the dots and the background. The Hough transformation might count the pixels that have low grey value but do not belong to a dot into the Hough circle of that dot. In Fig. 27, two dots, one close to the dark region (dot 1) the other one far away from the dark region (dot 2), were chosen and analyzed using ImageJ. The absolute value of the slope in brightness of dot 1 is less than that of dot 2, therefore, the Hough circle of the dot closer to the dark region would be larger than the actual dot and results in higher

permeability. Less Y takes less H atoms to form equilibrium hydride, therefore the dots would expand faster at which the Y is thin. Theoretically the permeability values in the figure X should all be the same because the permeability of a pure material should be constant and thickness-independent. The permeability reported at the center of the substrate is 1.66×10^{9}mol/m/s/Pa$^{0.5}$. Our result is close to the permeability value reported in bulk Pd (1.4×10^{-9}mol/m/s/Pa$^{0.5}$) [12], but is two times less than the value reported in Pd thin film (3.4×10^{-9}mol/m/s/Pa$^{0.5}$) [13].

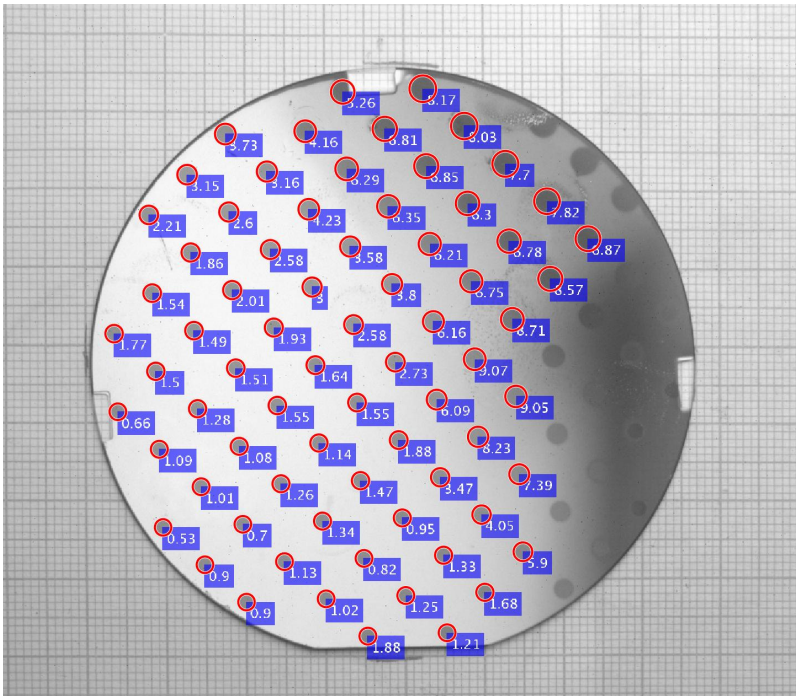

Fig. 25 The hydrogen permeability calculated for each dot on Pd sample 1. The values are reported in $1x10^{-9}$mol/m/s/Pa$^{0.5}$.

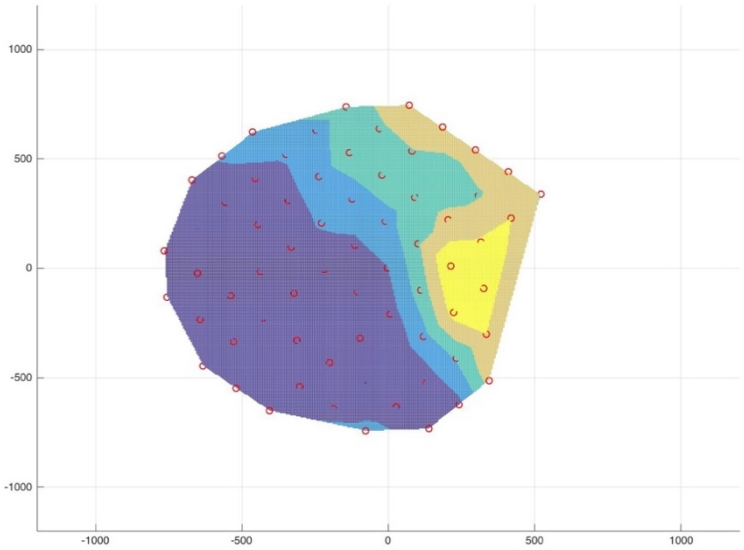

Fig. 26 The hydrogen permeability mapping of Pd sample 1. Brighter color represents higher permeability.

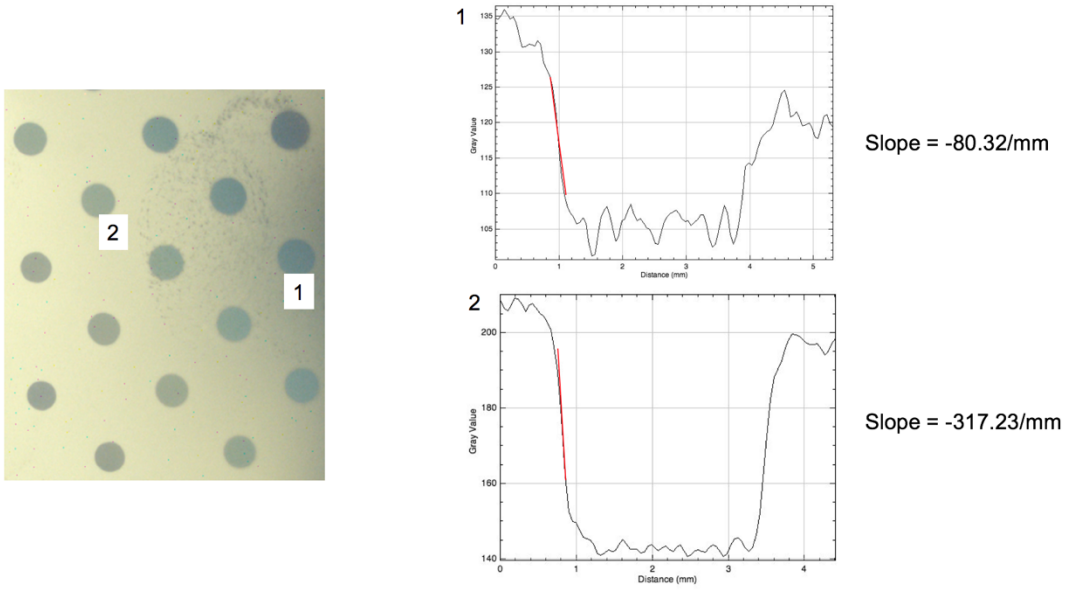

Fig. 27 Dot 1 is close to the dark region, dot 2 is away from the dark region. The brightness slope of the two dots were calculated

The hydrogen permeability in thin film Pd is reported to be faster than that in bulk Pd, which can be explained by the microstructure difference between the two. The grains in bulk metal typically have sizes in the order of micrometers while the grains in thin

films are generally less than the thickness of that thin film (less than 80nm in this cases). Therefore, more grain boundaries exist in thin film Pd. Although the H atoms uses interstitial diffusion as the main diffusion mechanism, having more grain boundaries would still facilitate the diffusion.

The permeability calculation (Eq. 3) is mainly affected by three factors: the thickness of test material, the thickness of indicator, and the exposure time. The deposition rate of Y and Pd at the center of the substrate were measured using the XTM during deposition, therefore the center thickness of each layer is well determined. The permeability calculated for the center dot is less than the literature value, which suggests that the recorded exposure time might be longer than the actual exposure time. The pure Pd sample 1 was originally made not to calculate the permeability but to test the validity of our method, so the exposure time was not carefully recorded. The Pd and Y layers on Pd sample 1 are not uniform as they were deposited from the side guns, and the thickness of each layer was approximated using the relative deposition rate. The hydrogen permeability is plotted against the thickness of Y and Pd layers in figure 28. In Fig. 28(a) the apparent hydrogen permeability decreases with the increase in Y thickness until the thickness reaches 80nm, and in Fig. 28(b) the permeability increases with the increase in Pd thickness. We expect the hydrogen permeability should be independent from the thickness of both layers, we speculate that the trend appears in Fig. 28 is due to error in our thickness estimation.

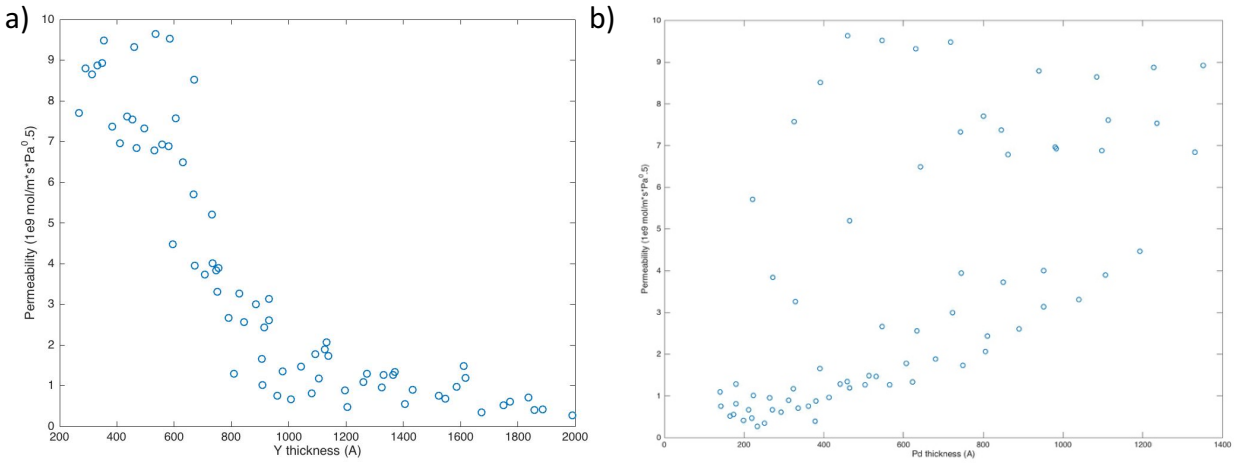

Fig. 28 (a) Hydrogen permeability plotted against the thickness of Y for Pd sample 1. (b) Hydrogen permeability plotted against the thickness of Pd for Pd sample 1.

3.2.1.2 Gradient Pd on uniform Y

Another pure Pd sample was deposited and processed to further investigate the validity of the method (Pd sample 2). In Pd sample 2, Y was deposited from the center gun of the 4-gun cluster (80nm at the center), and the Pd was deposited from gun 2 (45nm at the center). The thickness of Y should be relatively uniform and the thickness of Pd should be symmetric about the vertical axis, thus the overall thickness of the metals layers should be vertically symmetric as well. The nitride layer has a relatively uniform thickness as it was deposited from the 4-inch gun (55nm at the center). The sample was patterned using photolithography, but etched only by ion milling for 45 seconds to remove the nitride. No CF_4 etching was involved because we were trying to investigate the etch rate of nitride in the ion mill to develop an etching method for samples contain materials not allowed in the CF_4 dry etcher, such as samples containing Au and Ag.

The sample was exposed to 5% H_2 gas for 18 hours, a picture of the indicator was taken and processed for analysis (Fig. 29). We introduced the gas diffuser into the glass furnace when exposing Pd sample 2, so it was unexpected to see that H atoms diffused through the nitride cover on the lower left part of the substrate. Our hypothesis is that there are some micro-cracks on the nitride, which are large and deep enough for H_2 molecules to diffuse through and contact the Pd. White dots appeared on the lower right and inside the dark area on the lower left. The white dots show a clear sign of over etching, because all the metals on those dots were etched off and the white color comes from the grid paper behind the substrate. One might also notice that there are more white dots on the lower left than on the lower right, which suggests either the ion milling was non-uniform or the thickness of the thickness of metal layers if not symmetric. The ion mill has a large plasma source and the substrate is close to the ion gun during etching, so the etching is expected to be highly uniform. The thickness symmetry issue will be discussed with the permeability calculation.

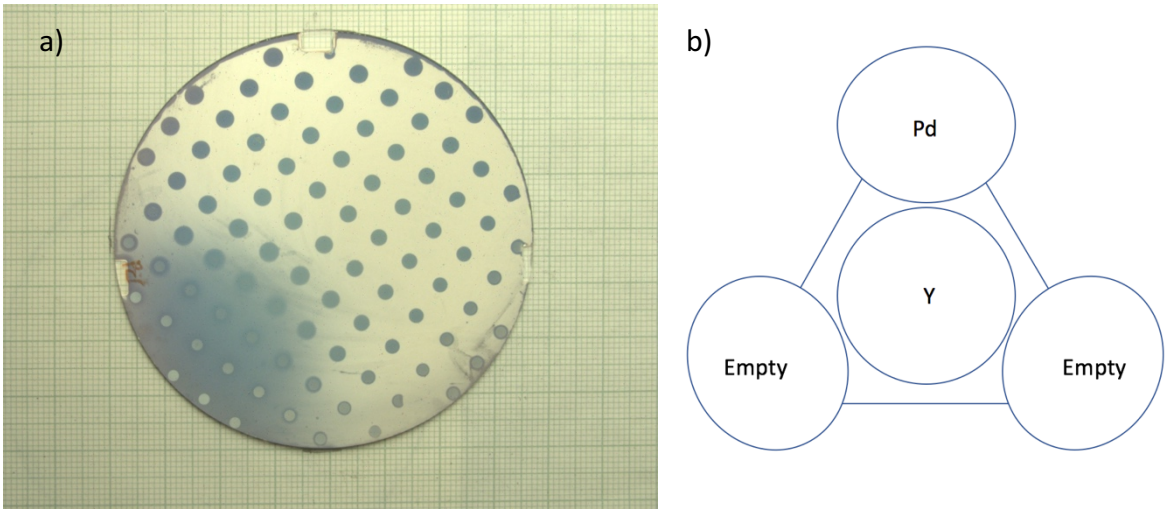

Fig. 29 (a) Image of the indicator side of the Pd sample 2. (b) Setup of the sputter guns in the 4-gun cluster

The hydrogen permeability of each dot is reported in units of $1x10^{-9}$ mol/m/s/$Pa^{0.5}$ in Fig. 30 and the Hough circles are shown in figure 28. Most dots have permeability in the range between $3\sim4x10^{-9}$ mol/m/s/$Pa^{0.5}$, which is constant with the hydrogen permeability recorded in literature for Pd thin films [13]. The dots around the dark area have permeability way higher than the rest of the dots, which is the same problem observed in Pd sample 1 and is due to the poor contrast between the dots and background. Three dots were chosen and measured with ImageJ, among which dot 1 is the closest to the dark region and dot 3 is the furthest away from the dark region. The absolute value for brightness slope of dot 1 is much less than that of dot 3, thus it is likely for the Hough circle of dot 1 to be larger than the size of the actual dot.

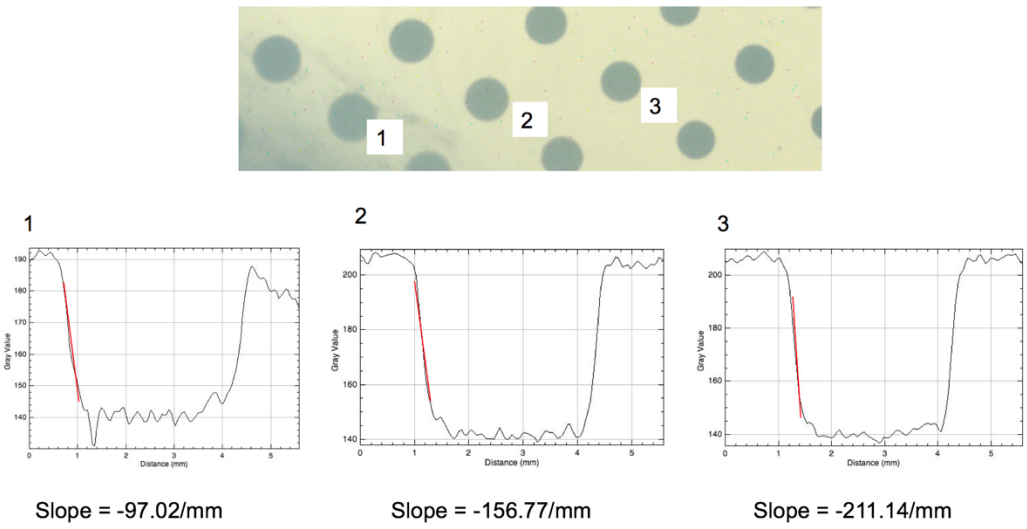

Fig. 30 Dot 1 is the closest to the dark region while dot 3 is the furthest. The brightness slope of the three dots were calculated

The permeability values were shown in Fig. 31. The dot at the center, where the thickness of each layer was best known, has a permeability of $6.12x10^{-9}$mol/m/s/$Pa^{0.5}$, which almost two times higher than the literature value for Pd thin films []. The

hydrogen permeability of the center dot in Pd sample 1 and in Pd sample 2 are very different. The low center dot permeability in sample 1 can be explained by the misreported exposure time, and we think the high permeability of the center in sample 2 could also be explained by the influence of the dark area on the lower left.

In Fig. 32, the size of Hough circle of the center dot appears to be larger than the Hough circles above and to the right of it. However, the dots located closer to the top of the substrate should have larger sizes because thicker Pd has higher hydrogen permeance and the dots would expand faster. The Pd thickness gradient (Fig. 26) suggests that there is little change in Pd thickness of the horizontally neighboring dots, hence there should be little change in the size of Hough circles. However, the Hough circle of the center dot is 8% larger than its neighboring dots on the right. Thus, the high hydrogen permeability of the center dot was not an error of our algorithm, but is due to the influence of the dark area at the lower left. Using the surrounding dots as a reference, a reasonable permeability for the center is deduced to be around 5.8×10^{-9} mol/m/s/$Pa^{0.5}$.

It is also observed that the sizes of the dots on the right of the substrate are generally smaller than the sizes of the dots located on the left. The thickness of Pd deposited from gun 2 should be vertically symmetric, thus the size of Hough circles should also be vertically symmetric. Fig. 29(a) shows that more white dots appear on the lower left part of the substrate, which means the metal layers are thinner on the left. The placement of the side guns has determined that the deposition rate of the species deposited from the side should be mirror symmetric relative to the vertical center lines

of the substrate. Our thickness model is vertically symmetric, but the main problem with it is that we don't know the gradient of how thickness decreases as it moves away from the target. The thickness calculated using our model might not be accurate because we don't exactly know the slope of thickness changing along the deposition direction, but theoretically the calculated thickness distribution should be a good fit to the actual thickness profile. The fact that the overall thickness for Pd sample 2 is vertically asymmetric suggests that it is affected by some unknown factor. The cause of this problem is unknown, but one possibility is that the Y underlayer was not as uniform as we expect, which affects the thickness profile of the metal layers deposited on it.

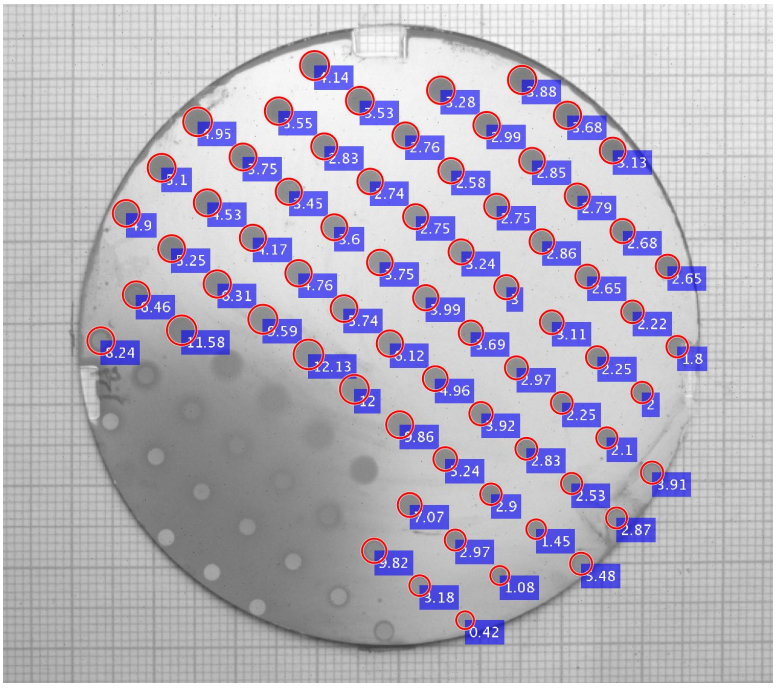

Fig. 31 The hydrogen permeability calculated for each dot on Pd sample 2.

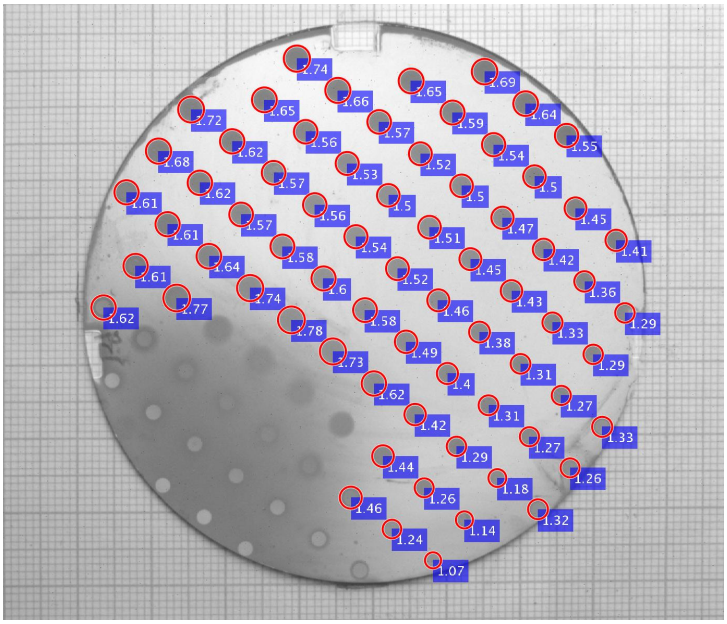

Fig. 32 Hough transformation result for the dots on Pd sample 2.

As a conclusion, the experiments performed on the two pure Pd samples show that the Hough transformation is a powerful tool for dot size analysis. Majority of the dots can be identified, except those that have irregular shapes and those that have poor contrast with the background. The radii measured using Hough transformation are close to the actual radii of the dots measured using ImageJ, which confirms the validity of Hough transformation. Our permeability calculation shows that the hydrogen permeability varies within pure Pd, which is not reasonable because the permeability of a pure material should be constant and independent from exposure time and thickness of each layer. Our thickness model doesn't work so well at predicting how thickness varies along the deposition direction, but the model itself is vertically symmetric and should be a good representation of the thickness distribution of a species deposited from the side gun. The asymmetric thickness behavior on Pd sample 2 is due to some unknown factor and two possibilities were discussed.

3.2.2 Palladium copper alloy

A sample with palladium copper alloy being the test material was deposited and tested. The Y indicator was deposited from gun 1, which has a center thickness of 80nm. The Pd was deposited from gun 2, and Cu was deposited from gun3. The composition at the center of the PdCu alloy was $Pd_{80}Cu_{20}$, and the center thickness of the test material was 110nm. The nitride layer was deposited from the 4-in gun with a center thickness of 35nm. The sample was patterned using photolithography, etched with CF_4 for 90 seconds, and etched with ion milling for 3 seconds to clean the exposed test material. The substrate was exposed in 5% H_2 gas for 9 hours. The processed image of the sample after exposure is shown in Fig. 33(a), and the setup of sputter guns is shown in Fig. 33(b). A fraction of the substrate to the right of the black line turned blue, which was caused by deposition instead of the H_2 exposure. The Y was deposited from the gun 1, and the thickness of Y at the blue area was thinner than the center of the substrate and takes less H atoms to form equilibrium hydride. During deposition, the Ar plasma not only knocks off Pd and Cu from the target, but also breaks the residual water molecules inside the deposition chamber into H and O atoms. The test material was deposited from gun 2 and gun 3, so there was a stronger intensity of Ar plasma and a higher local concentration of H atoms at the lower half of the substrate. Thin Y and high H atom concentration are the reasons for the right part of the substrate to turn blue even before the sample been exposed to H_2 gas.

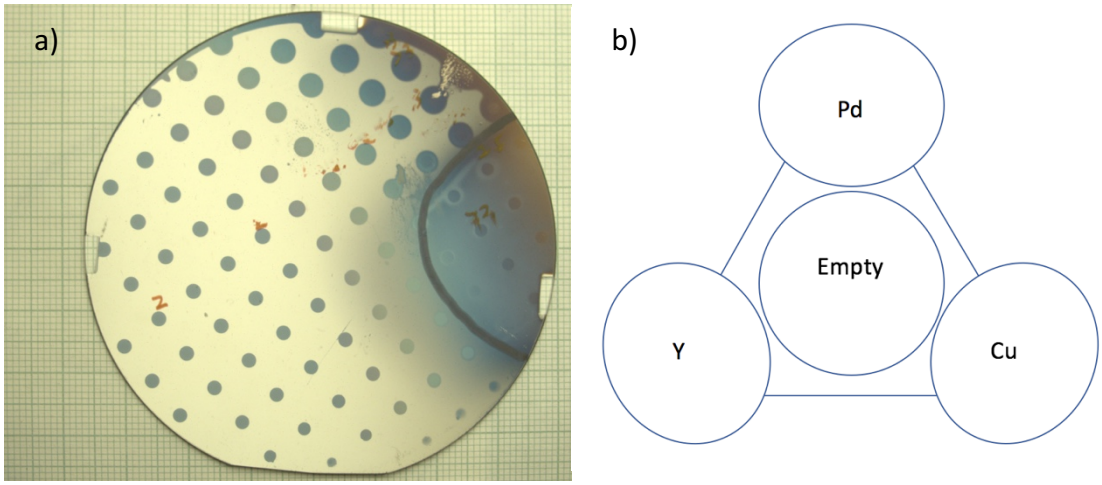

Fig. 33 (a) Processed image of the PdCu sample with center composition of $Pd_{80}Cu_{20}$. (b) The sputter gun setup of the 4-gun cluster.

The result for Hough transformation is shown in Fig. 34, and the radius of each dot was presented in centimeters. Most of the dots were detected by the Hough transformation, except those that have irregular shapes and those have poor contrast with the background. The dots are larger at the top of the substrate, where the Pd concentration is higher, and size decreases as at it moves away from where the Pd was deposited. One dot on the very top of the substrate has a measured radius of 0.153cm, which much less than its actual size although the dot itself is incomplete due to the hydrogen atoms infiltrated form the edge of the substrate. Hydrogen infiltration affected several dots located at the top of the substrate due the thin Y and the long exposure time. Some dots on the lower right of the substrate are incomplete, which indicates that that the hydrogen dissociation ability of the Pd alloy was prohibited when the Cu concentration is too high.

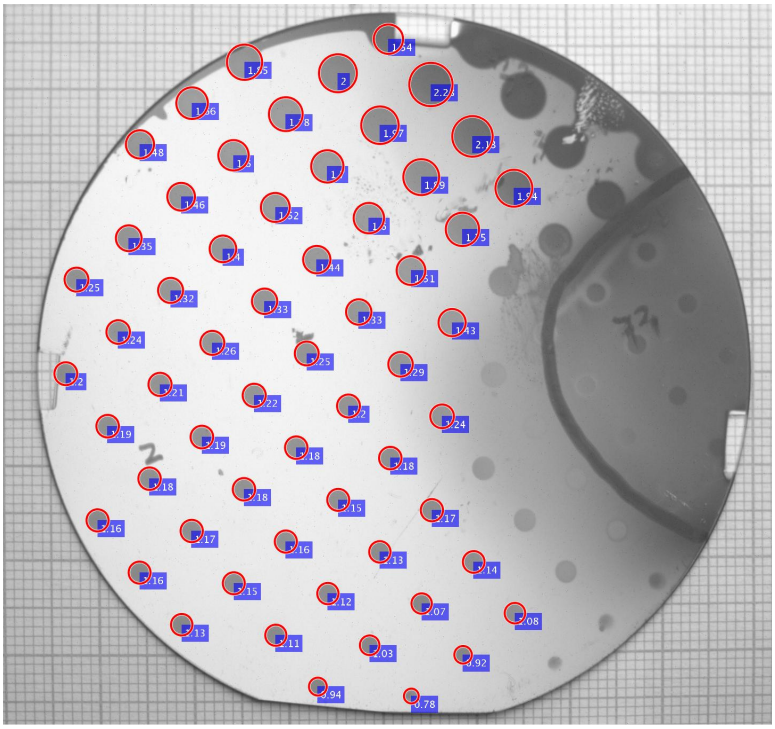

Fig. 34 Hough transformation result fot the PdCu sample with center composition of $Pd_{80}Cu_{20}$.

The permeability of each dot is calculated and shown in Fig. 35, in which the values are presented in units of $1x10^{-9}$mol/m/s/$Pa^{0.5}$. The highest permeability shown on Fig. 35 is $8.53x10^{-9}$mol/m/s/$Pa^{0.5}$, much higher than the hydrogen permeability calculated for the pure Pd sample 2 and could be the problem related to uncertainties in the thickness measurement. The permeability of $Pd_{80}Cu_{20}$ (the composition at the center of the substrate) was calculated to be $1.44x10^{-9}$mol/m/s/$Pa^{0.5}$, while the dots that have 40at.% to 60at.%Pd have permeability range between $1\sim2x10^{-9}$mol/m/s/$Pa^{0.5}$. The hydrogen permeability of PdCu thin film is with around 50 at.%Pd is reported to be higher than $6x10^{-9}$mol/m/s/$Pa^{0.5}$ in literature[14], therefore our permeability result is low compared to the values in the literature. Assuming there is no error in the exposure time, the actual thickness of the PdCu thin film is 3 times less than the calculated thickness. However, the thickness at the center of a sample is well

determined as we know the deposition rate and deposition time. There might be some interaction between the Cu and Pd atoms during deposition so that the material landed on Y indicator is less than what shows on the XTM. The permeability mapping is shown in Fig. 36(a) and the permeability of the dots is plotted against the Pd concentration in Fig. 36(b). It is clear that the hydrogen permeability in PdCu alloy increases with the Pd concentration, and that the dissociation or diffusion is shut down for the dots with less than 20 at.%Pd. PdCu alloy forms a two phase structure at room temperature because Pd and Cu are not miscible according to the phase diagram of PdCu system. Cu atoms might segregate around the Pd atoms the Cu concentration is higher than 80 at.%. When this phenomenon happens on the surface of PdCu thin film, not enough Pd atoms are in contact with H_2, which slows down or terminates the hydrogen dissociation reaction.

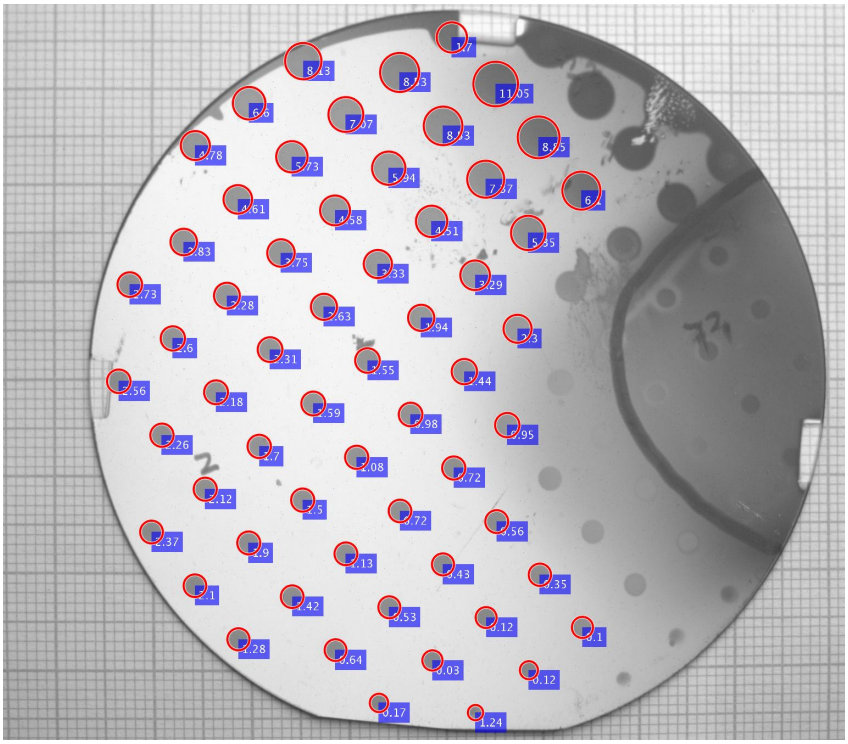

Fig. 35 Hydrogen permeability calculated for each dot on the PdCu sample with center composition of $Pd_{80}Cu_{20}$.

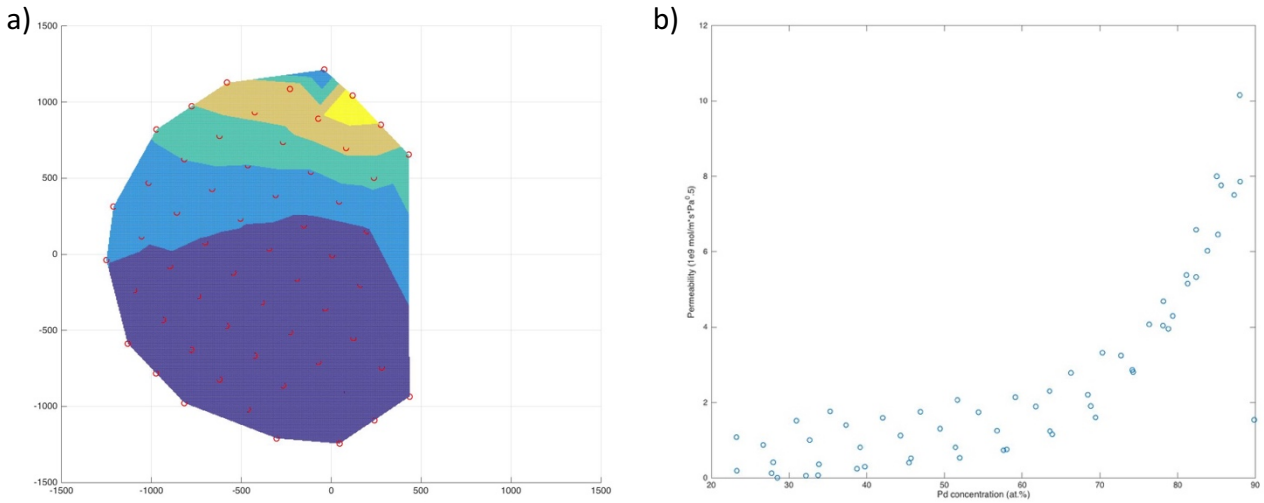

Fig. 36 (a) Permeability mapping for PdCu sample. (b) Hydrogen permeability plotted against the Pd concentration.

Another PdCu sample was prepared and tested to investigate the behavior of the PdCu alloy, mainly to check the critical Pd concentration needed to maintain the hydrogen dissociation at the surface of test material. The new sample was fabricated with the same sputter gun setup, same thickness for each layer, same processing method as the previous sample, and the same exposure time to the H_2 gas. The only difference is that the composition at the center of the test material changed from $Pd_{80}Cu_{20}$ to $Pd_{60}Cu_{40}$. The Pd concentration of each Hough circle is shown in Fig. 37. A fraction of the substrate turned blue before the sample was exposed to H_2 gas for the reason discussed earlier. We infer observed that the dissociation reaction was shut down on the PdCu surface with less than 20 at.%Pd, which is consistent with the result we observed from the previous sample. This shows that the effect in one of the composition rather than geometry of the sputtering deposition (which might have affected structure) or the configuration for exposure to H_2. The permeability of each dot was plotted against the

Pd concentration in Fig. 38. In the new sample the permeability of the substrate at around 80 at.%Pd was around $6x10^{-9}$mol/m/s/$Pa^{0.5}$, and is consistent with the result shown in Fig. 36(b).

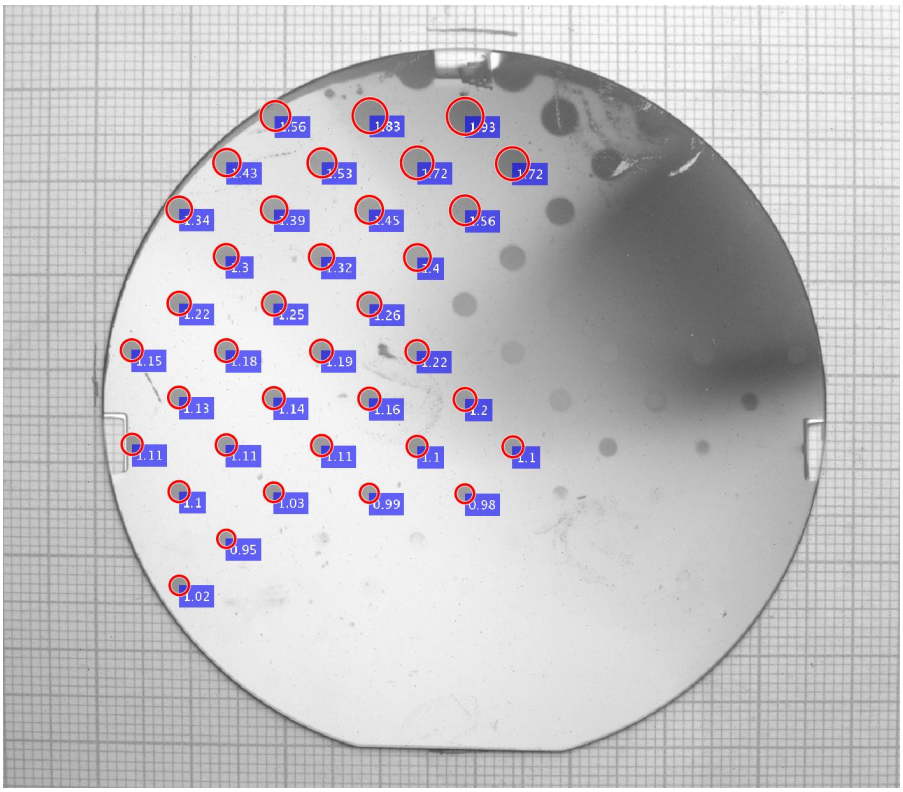

Fig. 37 Hough circles detected on the new PdCu sample with the Pd concentration reported in at.% for each dot.

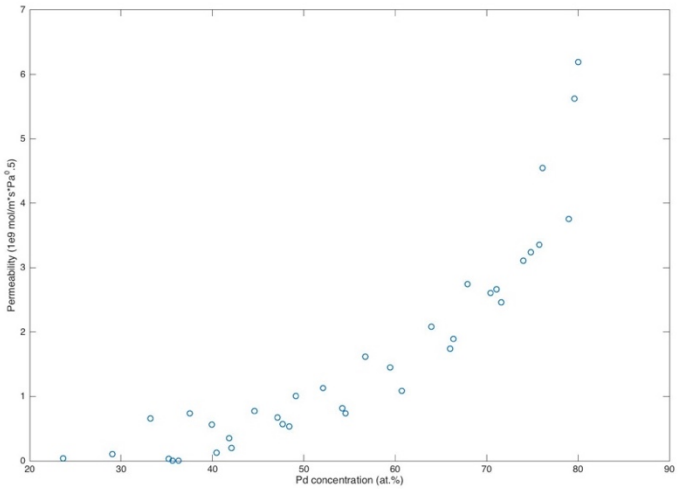

Fig. 38 The plot of hydrogen permeability of each dot on the new PdCu sample against the Pd concentration.

Our result from the two PdCu samples agree with each other in terms of the critical Pd concentration required to maintain hydrogen dissociation reaction. The dots on different sample but have the same alloy composition have the same calculated permeability, which again shows that the algorithm is consistent between the samples. Our algorithm may not be good enough to give quantitative results to compare to with the literature, but works well to provide qualitative results to find the optimum composition that exhibits highest hydrogen permeability.

3.2.3 Palladium ruthenium alloy

A sample with palladium ruthenium alloy being the test material was deposited and tested because we are interested to see the catalysis ability of PdRu alloy of different compositions. The Y indicator was deposited from the center gun of the 4-gun cluster (80nm at the center of the substrate), Pd was deposited from gun 2, Ru was deposited from gun 3, and the nitride layer was deposited from the 4-in gun (55nm at the center) as shown in Fig. 39(b). The center composition of PdRu alloy was 50 at.% Ru, and the center thickness of PdRu layer was 80nm. This sample was patterned using photolithography, etched with CF_4 for 90 seconds, and etched with ion milling for 3 seconds. The substrate was exposed in 5% H_2 gas for 6 hours. The processed image of the sample after exposure is shown in Fig. 39(a). On the left of the substrate some H_2 diffused through the nitride and a small fraction of the indicator turned blue. Some scratches appeared on the surface of the nitride after sample processing, which is the cause of the blue “scratches” on the indicator after exposure.

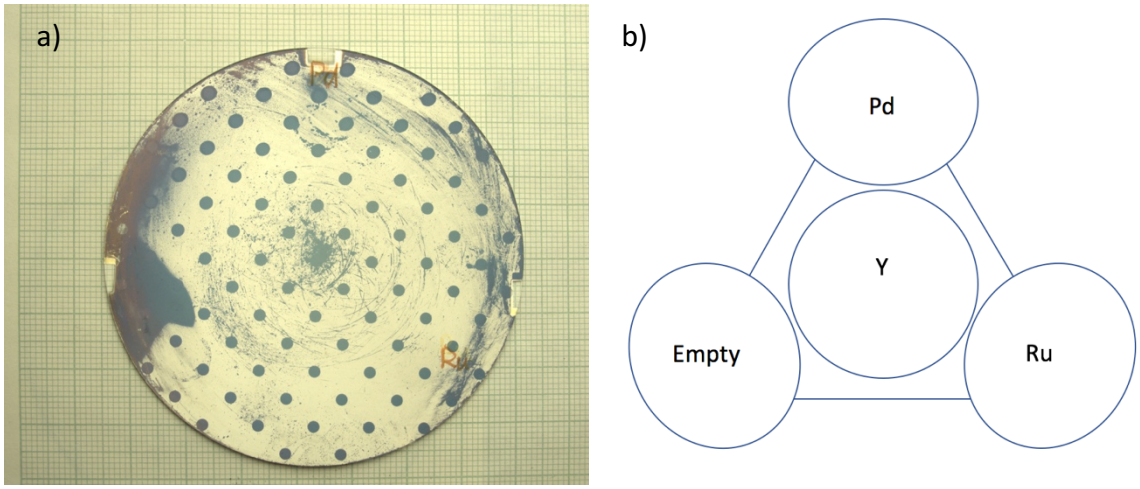

Fig. 39 (a) Processed image of the indicator side of PdRu sample. (b) The sputter gun setup of the 4-gun cluster.

The result of Hough transformation is shown in Fig. 40, in which the radii of dots are reported in centimeters. Although most of the dots are visible on Fig. 40, some were not identified as dots according to the Hough transformation. Those unidentified dots, like the one in the center of the substrate, are affected by the blue scratches and their shapes became irregular and no longer detectable. The dot size is larger at the top of the substrate, because thicker palladium has higher permeance. The largest dot appeared at the top left of the substrate, where there is the least Ru, while the smallest dot appeared at the bottom right of the substrate, where the Ru was deposited from. One could already notice from the Hough circles that the diffusion of hydrogen inside the alloy is heavily affected by the Ru concentration.

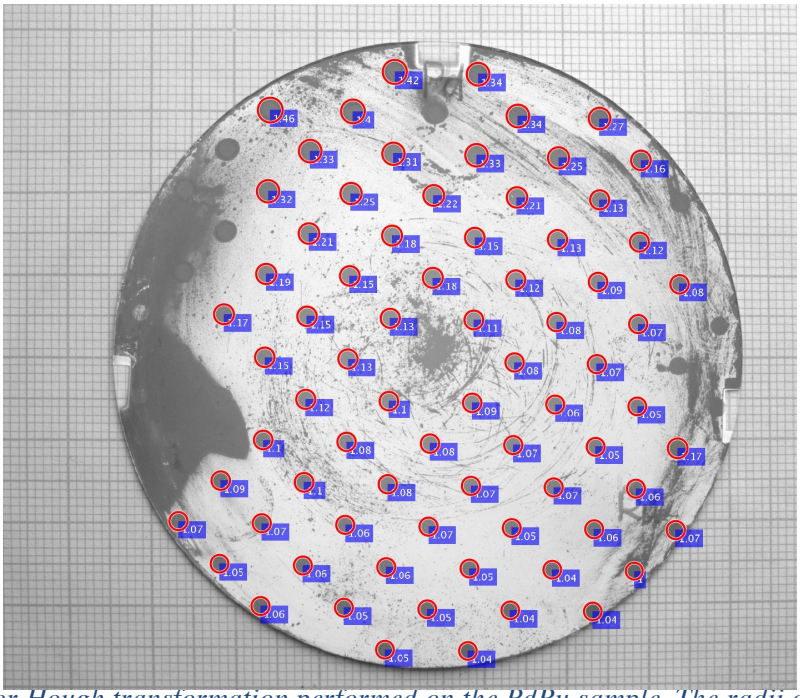

Fig. 40 Result for Hough transformation performed on the PdRu sample. The radii of the Hough circles are presented in centimeters.

The permeability of each dot was calculated, and the values are reported in Fig. 41 in $1x10^{-9}$mol/m/s/$Pa^{0.5}$, and the permeability mapping is shown in Fig. 42, in which higher permeability is represented by a brighter color. As expected the highest hydrogen permeability appeared at the top left part of the substrate and decreases towards the bottom left, where the Ru was deposited from. The highest permeability appeared on Fig. 42 is $5.88x1x10^{-9}$mol/m/s/$Pa^{0.5}$, a little bit higher than the hydrogen permeability of the center dot on Pd sample 2, which is deduced to be around $5.8x1x10^{-9}$mol/m/s/$Pa^{0.5}$.

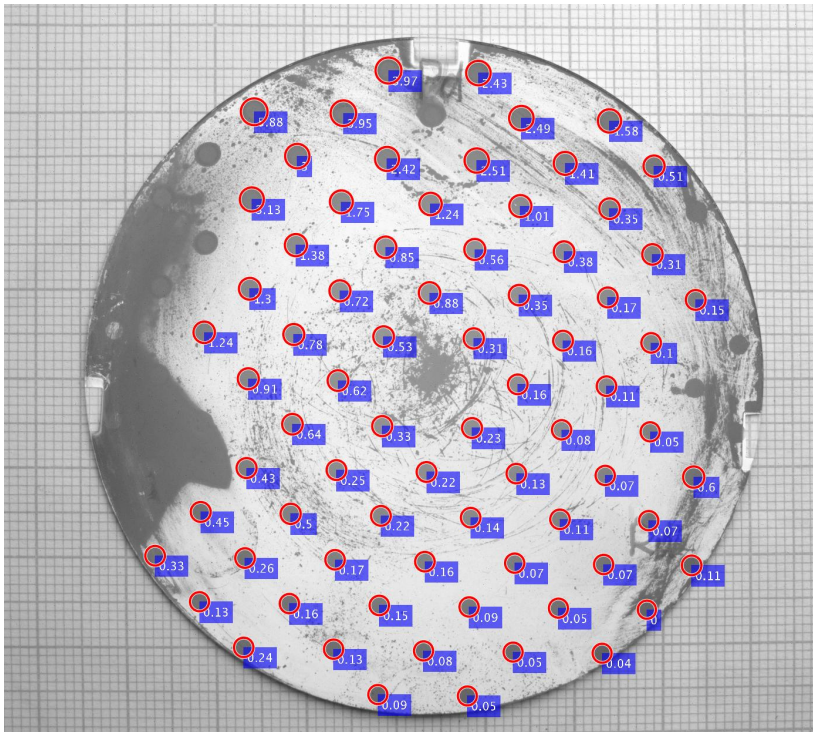

Fig. 41 The hydrogen permeability calculated for each dot on the PdRu sample.

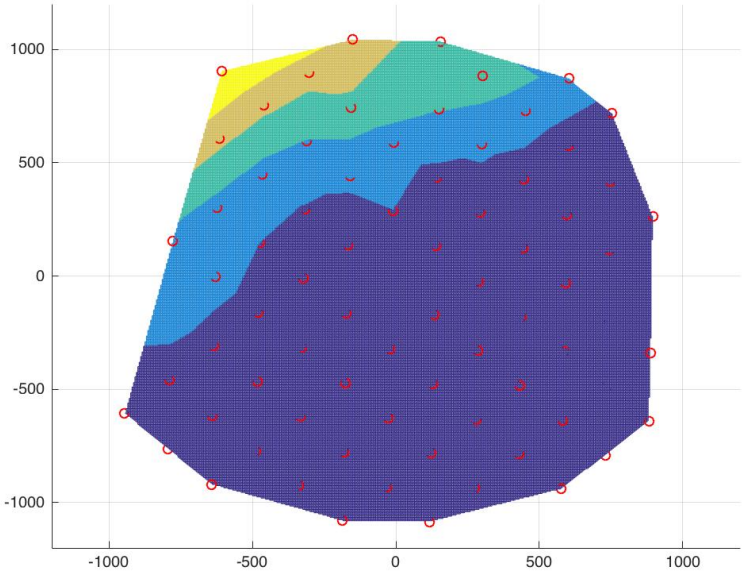

Fig. 42 The hydrogen permeability mapping for the PdRu sample.

The hydrogen permeability is plotted against the Ru concentration in Fig. 43, from which the highest permeability appeared at 10 at.%Ru and the value decreases as the Ru concentration increases. Hydrogen Permeability of PdRu alloy membrane with 10at.% Ru at 573K was found to be around $7.56x10^{-9}$mol/m/s/$Pa^{0.5}$ in literature. The permeability for the same alloy was recorded from 773K to 573K in the literature, from the permeability-temperature relationship the permeability at room temperature is calculated to be around $3.03x1x10^{-9}$mol/m/s/$Pa^{0.5}$, which is less than the literature value for pure Pd [15] and much lower than our result. It is reported that the maximum hydrogen permeability for PdRu alloy was found at 4.5at.%Ru. However, the lowest Ru concentration we synthesized on this substrate is 10at.%. To investigate PdRu alloy with lower Ru concentration we need try a different composition target for the substrate center. Since the hydrogen permeability appears to increase as the Ru concentration decreases, extrapolated permeability of PdRu alloy with lower Ru concentration to be higher than the permeability of pure Pd.

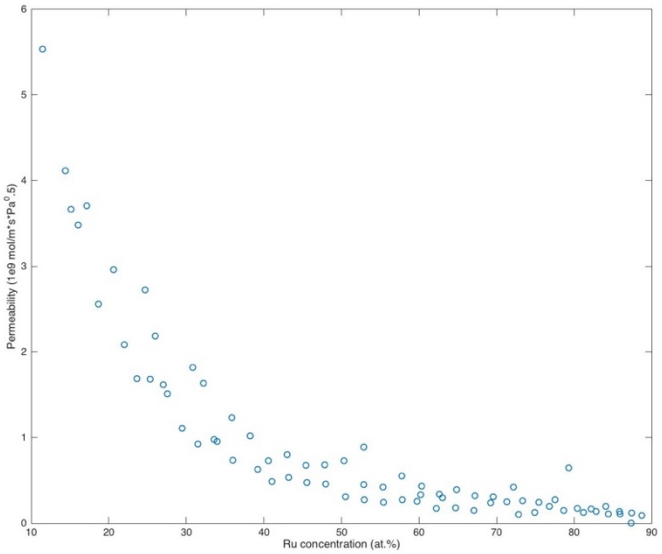

Fig. 43 The hydrogen permeability of each dot on the PdRu alloy is plotted against the Ru concentration

The accuracy of permeability calculation based on how well we know the thickness of the indicator and test material layers. It is discussed in section 3.2.1 that our thickness model is not an accurate match to the actual thickness profile of species deposited from the side guns, only at the center of the substrate is the thickness known accurately, since it was measured during deposition. With the uncertainties in thickness, the test material on the highest permeability dot might be thicker than what we have calculated so the actual permeability would be lower. The composition at each dot is also calculated using the thickness model: the amount of each species is calculated by dividing its thickness with its density, and the composition is calculated by diving the amount of one species with the amount of all species. Therefore, the Ru concentration at the dot with highest permeability might be lower than what we have calculated thus explaining its apparent high permeability.

3.2.4 Palladium molybdenum alloy

A sample with palladium molybdenum alloy being the test material was deposited and processed. The Y indicator was deposited from the center gun of the 4-gun cluster (80nm at the center of the substrate), Pd was deposited from gun 2, Mo was deposited from gun 1, and the nitride layer was deposited from the 4-in gun (55nm at the center). The center composition of PdMo alloy was 50 at.% Mo, and the center thickness of PdMo layer was 80nm. This sample was patterned using photolithography, etched with CF_4 for 90 seconds, and etched with ion milling for 3 seconds. The substrate was exposed in 5% H_2 gas for 6 hours, and a photo of the indicator side was taken. The

processed image of the sample after exposure is shown in Fig. 44(a), and the setup of sputter guns is shown in Fig. 44(b).

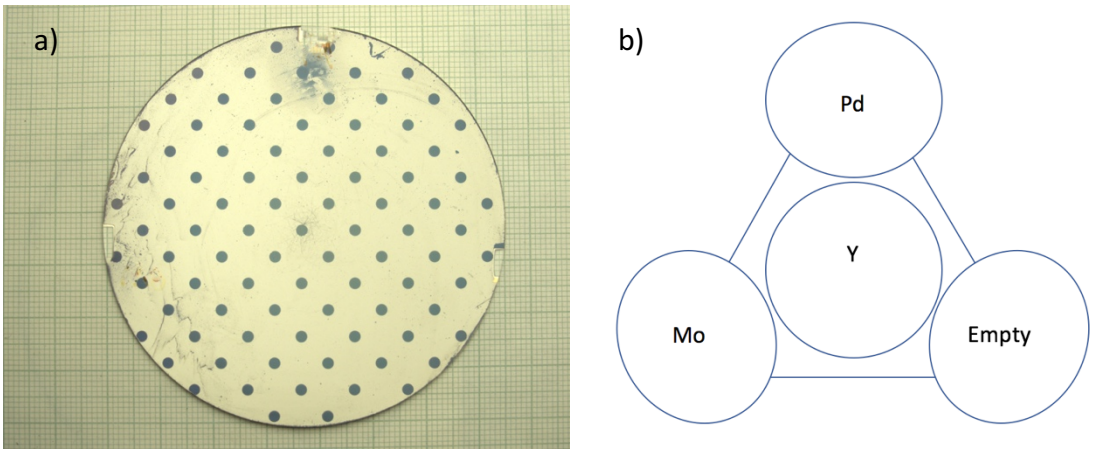

Fig. 44 (a) Processed image of the indicator side of PdMo sample. (b) The sputter gun setup of the 4-gun cluster.

The result for Hough transformation is shown in Fig. 45, and the radii of dots are shown in the figure in centimeters. Every dot appeared after exposure, while a tiny fraction of the indicator was affected by the hydrogen diffused through the nitride barrier. Hough transformation detected all the dots except one at the top of the substrate, which was surrounded by the blue color caused by hydrogen infiltration. The radii of all the dots appeared to be around 1.1mm, hence there is only 10% increase in dot size comparing to the size of holes patterned on the nitride, regardless of the Pd concentration of the corresponding test material. We have concluded from the previous samples that the dots under test material of higher Pd concentration should have larger sizes due to the high hydrogen permeability of Pd. The size of blue dots on the indicator is so close to the size of dots patterned on the nitride, which shows that the hydrogen dissociation ability of Pd is intact across the whole substrate.

However, the addition of Mo dramatically reduced the diffusion rate of hydrogen inside the alloy regardless of the concentration of Pd.

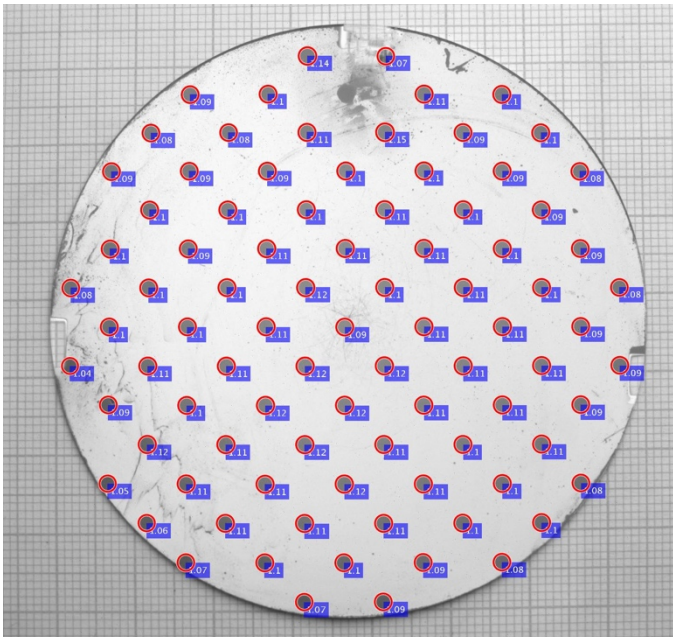

Fig. 45 The result of Hough transformation for the PdMo sample. The radii of the Hough circles are reported in centimeters.

The hydrogen permeability of each dot after the 6-hour exposure was calculated and shown in Fig. 46, the permeability values are reported in $1x10^{-9}$mol/m/s/$Pa^{0.5}$. The permeability value at the center of the substrate, where the thickness and composition of the alloy was accurately measured, was $0.25x10^{-9}$mol/m/s/$Pa^{0.5}$. The hydrogen permeability at the center is more than 15 times lower than the literature value for Pd thin film, and even less for the values we calculated with the pure Pd sample 2 (section 3.2.1.2). After the photo was taken and analyzed, this PdMo sample was returned to the glass furnace and exposed to 5% H_2 gas for another 60 hours, but no expansion on the dots were observed. 60 hours is enough for the dots to expand if H atoms are

entering the indicator, therefore, the hydrogen dissociation reaction is turned off at the surface of PdMo dots. Pd and Mo are immiscible at room temperature, and Mo has a lower surface energy comparing to Pd. It is possible that after some time the Mo atoms migrates towards the surface of the exposed test material, preventing H_2 from contacting Pd thus shut off the dissociation reaction. Even though Mo provides good resistance against corrosion, it is a poor additive to Pd to create a hydrogen separation membrane.

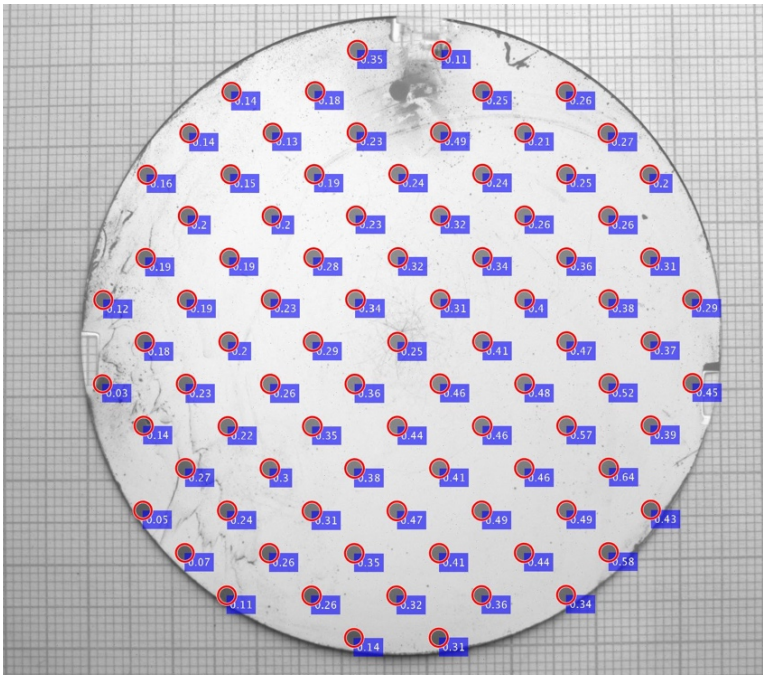

Fig. 46 The hydrogen permeability is calculated for each dot on the PdMo sample.

3.2.5 Palladium silver gold alloy

Palladium silver gold alloy was prepared as the test material. The Y indicator was deposited form the center gun of the 4-gun cluster (80nm at the center of the substrate), Pd was deposited from gun 2, Au was deposited from gun 1, and Ag was

deposited from gun 3. The composition at the center of the substrate is $Pd_{33}Ag_{33}Au_{33}$, with a center thickness of 80nm. The nitride was deposited from the 4-inch gun (55nm at the center). This sample was patterned using photolithography, etched solely with ion milling for 45 seconds because samples containing Ag and Au are not allowed in the CF_4 etching chamber. The substrate was exposed in 5% H_2 gas for 6 hours, and a photo of the indicator side was taken. The processed image of the sample after exposure is shown in Fig. 47(a), and the sputter gun setup is shown in Fig. 47(b).

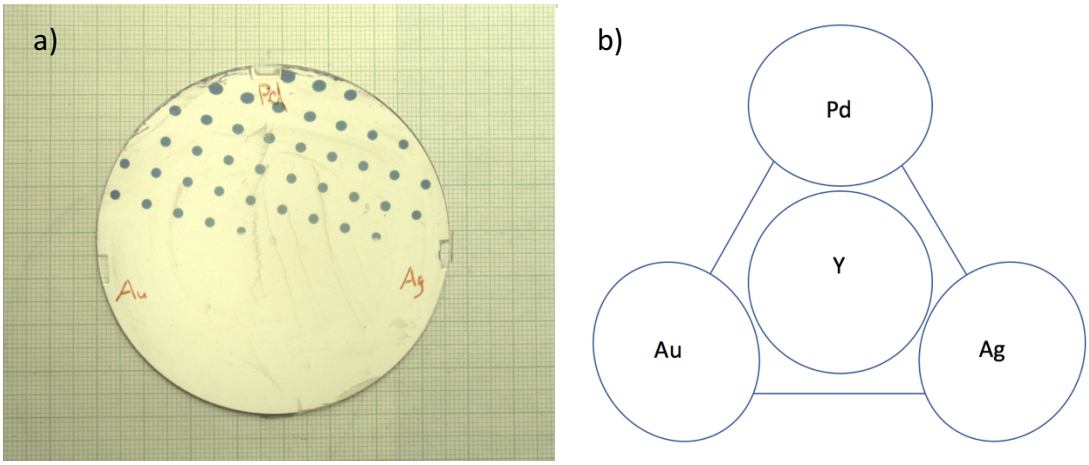

Fig. 47 (a) Processed image of the indicator side of PdAgAu sample. (b) The sputter gun setup of the 4-gun cluster.

The result of Hough transformation is shown in Fig. 48. The dots only appeared on the upper half of the substrate, but all the dots were detected by Hough transformation. As expected that the dots are larger for Pd-rich compositions and the size of dots decrease in regions where the Pd concentration is lower. The Pd concentration of each dot is shown in Fig. 49. Except the first three rows located at the top of the substrate, the size of all the other dots is very close to the size of the dots patterned on the nitride surface. The dots with less than 50at.%Pd experienced less than 10% expansion in their sizes,

which means the lateral diffusion of hydrogen of the corresponding alloy is negligible. Fig.48 shows that the hydrogen diffusion was completely shut down for the dots with less than 30at.%Pd. Either there is not enough Pd on the surface of exposed dots to dissociate H_2 molecules, or the diffusion rate inside the alloy is too low for the hydrogen atoms to reach the indicator and form hydride.

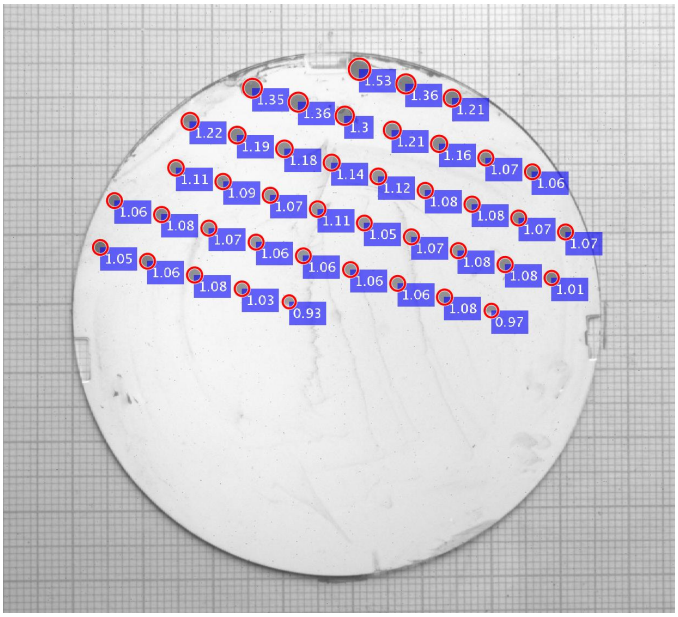

Fig. 48 The result for Hough transformation performed on the PdAgAu sample. The radii of Hough circles are reported in centimeters.

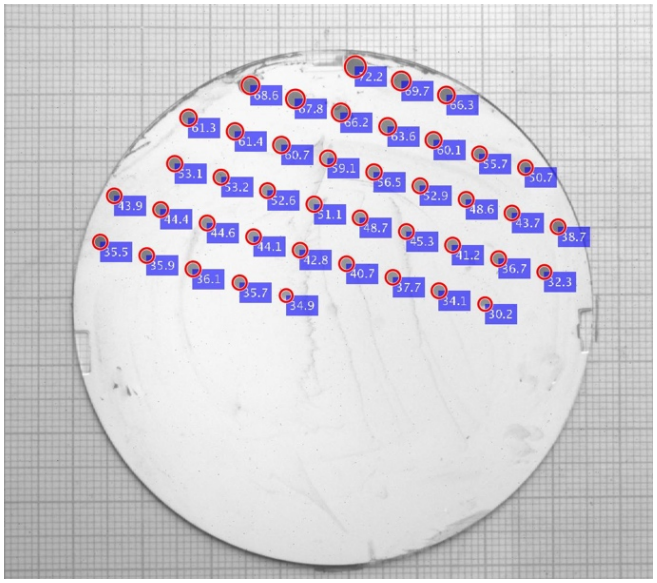

Fig. 49 The Pd concentration of each Hough circle presented in at.%Pd

We had the suspicion that the hydrogen dissociation ability of the alloy on the lower half of the substrate was impaired by the etching process, which left contaminants on the exposed dots on the lower half of the substrate. A sample was deposited the with the same set up as the sample presented above, except no nitride was deposited on the new sample, therefore no etching was required expose the test material. The new sample was exposed in 5% H_2 for 6 hours, and a photo of the indicator side was taken, processed, and shown in Fig. 50. The new sample was broken accidentally, so the pieces were not exposed identically. The blue area on the new sample is very close to the area in which the dots appeared on the old sample, which proves that having enough Pd is necessary for the dissociation of H_2 molecules and the diffusion of H atoms inside the alloy. Fig. 50 also shows that the addition of Au inhibited the dissociation of hydrogen at the surface of the Pd alloy than Ag did, because a larger fraction of the Ag rich area changed color than the Au rich area.

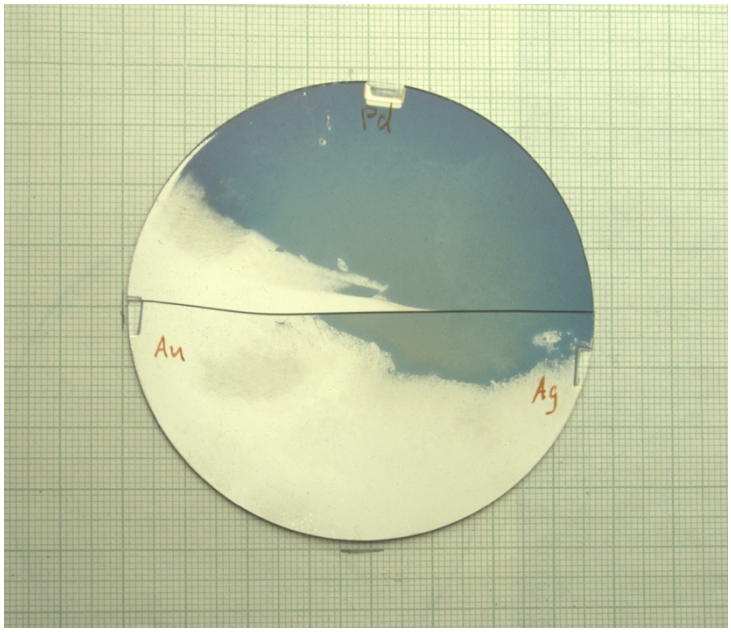

Fig. 50 The indicator side of a PdAgAu sample after 6 hours of exposure to 5% H_2 gas. Note that no nitride has been deposited on this sample.

The permeability of each dot was calculated and reported in $1x10^{-9}$mol/m/s/$Pa^{0.5}$ in Fig. 51. The permeability mapping is shown in Fig. 52(a), and the permeability was plotted against the Pd concentration in Fig. 52(b). It can be observed that the permeability of dots decreases dramatically with decreased concentration of Pd, and the highest permeability ($5.2x10^{-9}$mol/m/s/$Pa^{0.5}$) appeared at around 72at.%Pd. It was reported in literature that the addition of Ag in Pd facilitates the permeation of hydrogen at elevated temperature, and the maximum hydrogen permeability was found to be $6x10^{-9}$mol/m/s/$Pa^{0.5}$ at $Pd_{74}Ag_{26}$ at 400 ºC, which is higher than the permeability of pure Pd at that temperature [13]. The permeability in our sample is lower than literature not only because our sample was tested at room temperature, but also with the addition of Au seems to prohibit either the hydrogen dissociation ability or the hydrogen diffusion ability of the Pd alloy.

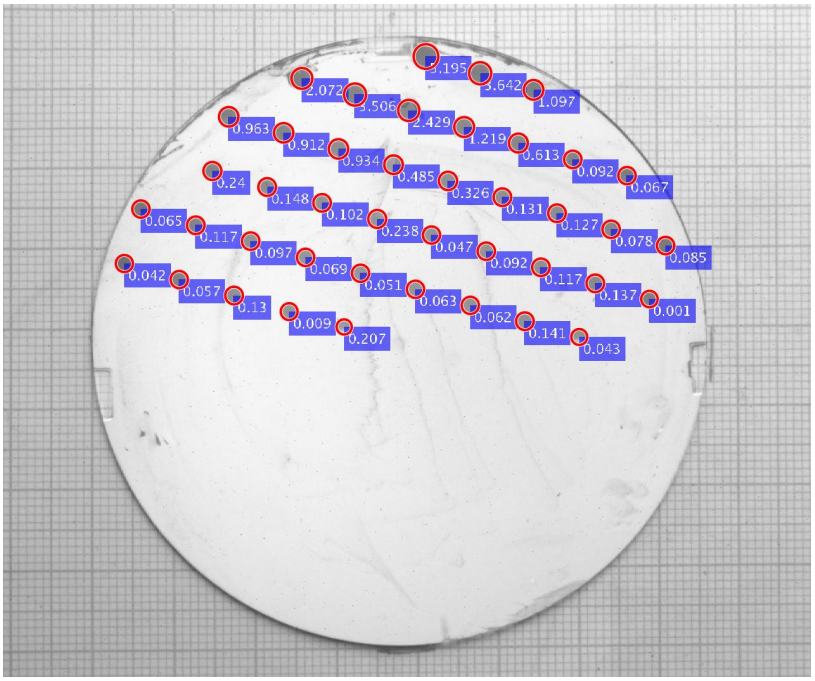

Fig. 51 The hydrogen permeability calculated for each dot on the PdAgAu sample.

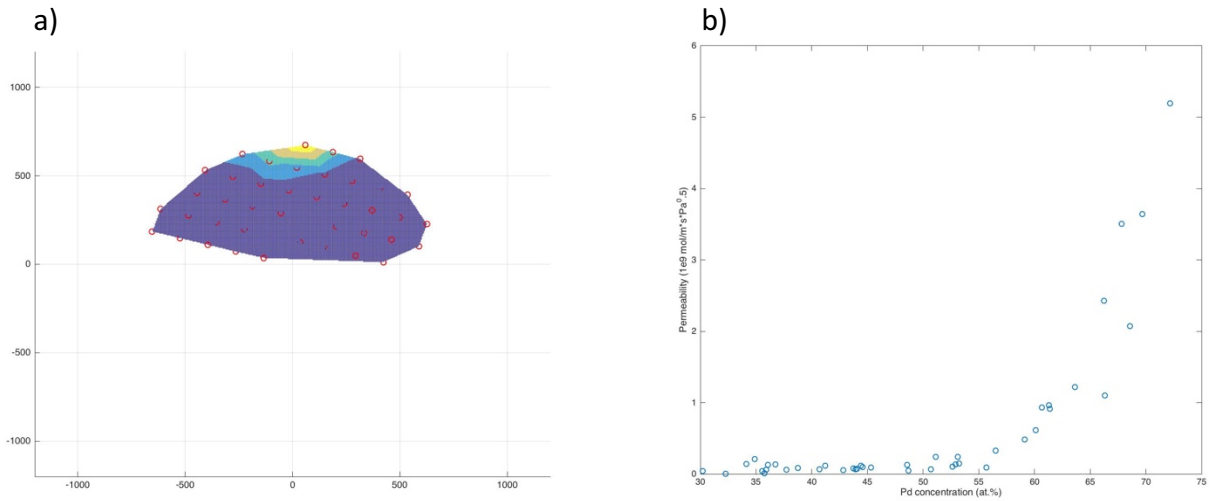

Fig. 52 (a) Permeability mapping for PdAgAu sample. (b) Hydrogen permeability plotted against the Pd concentration.

4. Conclusion

A new method that allows parallel analysis of a multitude of compositions of Pd alloys have been developed and presented. The validity of our method was tested using pure Pd, while the results for PdCu, PdRu, PdMo, and PdAgAu alloys are presented. In general, alloy with higher Pd concentration exhibits higher hydrogen permeability. It is discovered that for PdCu and PdAgAu alloy the hydrogen dissociation reaction at the sample surface was turned off when Pd concentration drops below a certain level, and it PdMo the hydrogen dissociation reaction at the surface stops after a certain amount of time.

Hough transformation has been proven to be a powerful tool in dot size measurement, since the Hough circles fits the dots well and the Hough radii is generally close to the size of the actual dots. It is also recognized that the calculated thickness of each layer using our thickness model might be different from their actual thickness, while the layer thickness is observed to be under the influence of some unknown factor during deposition like shown in pure Pd sample 2.

Overall, our method may not give good quantitative results on the hydrogen permeability since our numbers are not in total agreement with the literature values, but it provides quick, qualitative results on a wide range of alloy compositions.

5. Future Directions

The alternative method for hydrogen permeability measurement presented in this thesis is close to completion, but some problems still await to be solved. The silicon nitride barrier sometimes fails to block H_2 from contacting the test material under its cover, which can cause serious problems during the data analysis process. Therefore, it is important for us to find an alternative that serve as a good hydrogen barrier and can be etched without acid. It would be important to develop a better understanding on the difference between the layer thickness predicted by our thickness model and the actual layer thickness, so that the uncertainty in thickness prediction can be reduced and the accuracy in permeability can be improved. It would also be important for us to figure out the cause of thickness asymmetry appeared on pure Pd sample 2 and understand whether it is a random or re-occurring error.

It has been shown that the size of Hough circles for the dots around the dark areas on the indicator can be larger than the size of actual dots due to the poor contrast between the dots and the background. It would be important for us to improve the Hough transformation algorithm so that dot size detection requires no manual involvement. At last, it is necessary to develop a hydrogen permeability calculation algorithm which fits our sample setup and can give quantitative results that agree with the literature values.

6. Reference

[1] B.N. Lukyanov et al., Catalytic reactors with hydrogen permeation membrane separation, Chem. Eng. J. 154 (2009) 258-266.

[2] J.D. Figueroa, et al., Advances in CO2 capture technology – The U.S. Department of Energy's Carbon Sequestration Program, Int. J. Greenh. Gas Control. 2 (2008) 9-20.

[3] S. Yun, S.T. Oyama, Correlations in palladium membranes for hydrogen separation: A review, J. Membr. Sci. 375 (2011) 28-45.

[4] S.N. Paglieri, J.D. Way, Innovations in Palladium Membrane Research, Separ Purif Method, 31 (2002) 1-169.

[5] B.D. Morreale et al., The permeability of hydrogen in bulk palladium at elevated temperatures and pressures, J. Membr. Sci. 212 (2003) 87-97.

[6] R. A. Wach, M. Sugimoto, A. Idesaki, M. Yoshikawa, Molecular sieve SiC-based membrane for hydrogen separation produced by radiation curing of preceramic polymers, Materials Science and Engineering B 140 (2007) 81–89

[7] de Man et al., Combinatorial method for direct measurements of the intrinsic hydrogen permeability of separation membrane materials, J. Membr. Sci. 444 (2013) 70-76.

[8] George C. Yu, S.K. Yen, Hydrogen diffusion coefficient of silicon nitride thin films, Applied Surface Science 201 (2002) 204–207.

[9] Radoslaw A. Wach, Masaki Sugimoto, Akira Idesaki, Masahito Yoshikawa, Molecular sieve SiC-based membrane for hydrogen separation produced by radiation curing of preceramic polymers, Materials Science and Engineering: B, Volume 140, Issue 1, 2007, Pages 81-89

[10] Christopher Mizzi, Robert B. van Dover, High Throughput Method For Characterizing Pd Alloy Hydrogen Separation Membranes, Dept. of Materials Science and Engineering, Cornell University

[11] M.S. Whittingham, Hydrogen motion in oxides: from insulators to bronzes, Solid State Ionics. 168 (2004) 255-263.

[12] A. G. Knapton, Palladium Alloys for Hydrogen Diffusion Membranes, A Review of High Permeability Materials, Platinum Metals Rev., 1977, 21, (2), 44-50

[13] M.D. Dolan, Non-Pd BCC alloy membranes for industrial hydrogen separation, Journal of Membrane Science 362 (2010) 12–28

[14] R.J. Westerwaal, E.A. Bouman, W.G. Haije, H. Schreuders, S. Dutta, M.Y. Wu, C. Boelsma, P. Ngene, S. Basak, B. Dam, The hydrogen permeability of PdeCu based thin film membranes in relation to their structure: A combinatorial approach, International Journal of Hydroen energy 40 (2015) 3932-3943

[15] Sabina K. Gade, Matthew K. Keeling, Alexander P. Davidson, Oyvind Hatlevik, J. Douglas Way, Palladium–ruthenium membranes for hydrogen separation fabricated by electroless co-deposition, international journal of hydrogen energy 34 (2009) 6484–6491